



HAL
open science

Unveiling the transformation of 2,4,6-trihalophenols by active species in drinking water pipelines: The role of goethite

Feilong Dong, Jiani Zhu, Cong Li, Eric Lichtfouse, Wei Wang, Shuang Song

► **To cite this version:**

Feilong Dong, Jiani Zhu, Cong Li, Eric Lichtfouse, Wei Wang, et al.. Unveiling the transformation of 2,4,6-trihalophenols by active species in drinking water pipelines: The role of goethite. *Chemical Engineering Journal*, 2024, 492, pp.152390. 10.1016/j.cej.2024.152390 . hal-04586301

HAL Id: hal-04586301

<https://hal.science/hal-04586301v1>

Submitted on 24 May 2024

HAL is a multi-disciplinary open access archive for the deposit and dissemination of scientific research documents, whether they are published or not. The documents may come from teaching and research institutions in France or abroad, or from public or private research centers.

L'archive ouverte pluridisciplinaire **HAL**, est destinée au dépôt et à la diffusion de documents scientifiques de niveau recherche, publiés ou non, émanant des établissements d'enseignement et de recherche français ou étrangers, des laboratoires publics ou privés.

Public Domain

Unveiling the transformation of 2,4,6-trihalophenols by active species in drinking water pipelines: The role of goethite

Feilong Dong^{a,e}, Jiani Zhu^a, Cong Li^b, Eric Lichtfouse^c, Wei Wang^{d,*}, Shuang Song^{a,*}

^a College of Environment, Zhejiang University of Technology, Hangzhou 310014, China

^b School of Environment and Architecture, University of Shanghai for Science and Technology, Shanghai 200433, China

^c State Key Laboratory of Multiphase Flow in Power Engineering, Xi'an Jiaotong University, Xi'an, Shaanxi 710049, China

^d Department of Environmental Science, College of Environmental and Resource Sciences, Zhejiang University, Hangzhou 310058, China

^e Shaoxing Research Institute, Zhejiang University of Technology, Shaoxing 312085, China

ARTICLE INFO

Keywords:

Disinfection byproducts

Chlorination

Goethite

Free radicals

Transformation

ABSTRACT

The long-term accumulated pipe scale in the water distribution system (WDS) is vital for ensuring the safety of drinking water delivery. This study revealed a novel positive role of pipe scale in triggering interface free radicals for aromatic substances degradation. The goethite (main constituents of pipe scale) converts from the trivalent state to the divalent state by withdraw electrons from aromatic phenolic compounds. Active free radicals such as hydroxyl radical ($\cdot\text{OH}$), $\text{Cl}\cdot$, and $\text{ClO}\cdot$ were subsequently formed via a cascade of chain reactions under WDS conditions, among which $\cdot\text{OH}$ was the dominate active species driving efficient transformation of 2,4,6-trichlorophenol (60.8%) and 2,4,6-tribromophenol (80.5%) and the corresponding toxicity attenuation. The goethite mediated chlorination is a surface reaction following Langmuir–Hinshelwood model. Our works revealed the presence of natural source of $\cdot\text{OH}$ for disinfection byproducts transformation. Given the ubiquitous existence of iron scales inside ductile iron pipe, the finding renewed the understanding of the impact of WDS on drinking water quality.

1. Introduction

Disinfection byproducts (DBPs) persistently exist in tap water, primarily originating from the final disinfection processes in water treatment and continuing to be generated throughout the water distribution system (WDS). To date, more than 700 aromatic and aliphatic byproducts have been identified in drinking water [1]. In comparison to aliphatic DBPs such as trihalomethanes (THMs) and haloacetic acids (HAAs) with concentrations at the $\mu\text{g}/\text{L}$ level in drinking water, aromatic DBPs detected are typically 1 to 2 orders of magnitude lower [2]. Nonetheless, among various aromatic DBPs, 2,4,6-trihalophenols have received much attention to date since their cytotoxicity, developmental toxicity, and growth-inhibiting properties are tens to hundreds of factors higher when compared to numerous aliphatic halogenated DBPs and several halo-phenolic DBPs (e.g., halogenated hydroxybenzaldehyde and halogenated hydroxybenzoic acid) [3]. In which, 2,4,6-trichlorophenol (TCP) and 2,4,6-tribromophenol (TBP) are often found in drinking waters in China (ranging from 2.9 to 31.6 ng/L) [4]. In special, the highest concentration of TCP in the county of Ostergotland in

Sweden reached up to 640 ng/L in a tap-water sample [5]. Because of the high toxicity, persistent property and adverse impacts on environment and human health [6], TCP and TBP have been designated as priority pollutants in the USA and China [7,8].

Iron pipes are one of the extensively used materials in the WDS, but they are prone to form corrosion scale as a result of long-term use. Goethite is the predominant component of iron corrosion scales, comprising over 50 % of the iron minerals formed through corrosion processes [9–11]. It is composed of octahedral structural units consisting of $\text{FeO}_3(\text{OH})_3$. Goethite exhibits adsorption behavior towards chlorophenols by forming surface complexes. The hydroxyl groups present on the goethite surface can interact with the chlorophenols through hydrogen bonding or other electrostatic interactions [12,13]. This adsorption process allows goethite to effectively adsorb chlorophenols from aqueous solutions. Under pure and controlled conditions, it has been shown that adding synthetic goethite converts HClO into hydroxyl radicals ($\cdot\text{OH}$) via surface-initiated chain reaction similar to the Haber-Weiss Fenton process [14]. A single electron transfer from Fe(II) to HClO favors the generation of hydroxyl and chlorine radicals [15]. Therefore,

* Corresponding authors.

E-mail addresses: ww1@zju.edu.cn (W. Wang), ss@zjut.edu.cn (S. Song).

we hypothesized that radical formation could happen 'naturally' by reaction of Fe-enriched scale with aromatic phenolics. The $\bullet\text{OH}$ radicals are widely recognized as potent oxidizing agents, with sufficient power to decompose 2,4,6-trihalophenols through oxidative degradation [16].

The conversion of phenyl DBPs can proceed via electrophilic/nucleophilic substitution, oxidation–reduction reactions as well as decarboxylation [2]. The decomposition of 2,4,6-trihalophenols can generate small aliphatic DBPs (e.g., HAAs, THMs and haloacetonitriles) through two pathways involving ring opening and cleavage of the side chain [2]. Currently, research on the decomposition of aromatic DBPs primarily focuses on the disinfectant oxidation such as chlorination and chloramination. However, $\bullet\text{OH}$ radicals generated by goethite mediated chlorination alter the reaction between halogenated phenols and residual chlorine, leading to the more complex transformation pathway. Due to the presence of residual chlorine and goethite in the pipe network, the concentrations of 2,4,6-trihalophenols may vary with distance, thereby altering their impact on small aliphatic DBPs during delivery [17]. Understanding the transformation pathways of 2,4,6-trihalophenols based on goethite mediated $\bullet\text{OH}$ process can further reveal the mechanism of occurrence and transformation of DBPs, facilitating the development of strategies to control DBP formation.

In this work, we have demonstrated that the free radical process could spontaneously occur on goethite surface in the WDS. TCP and TBP were chosen as representative 2,4,6-trihalophenols to simulate the transformation of aromatic DBPs. The detailed mechanism of radical formation was elucidated through the use of radical scavenger and verified by instrumental analysis. The reaction kinetics was modeled based on the effect of processing variables. The degradation intermediates, potential degradation pathways and corresponding cytotoxicity were proposed.

2. Materials and methods

2.1. Chemicals and reagents

Goethite was obtained from Alfa Aesar Inc. (Ward Hill, USA). The X-ray powder diffraction (XRD) patterns reveals characteristic peaks that correspond to the distinctive crystal planes of goethite, which are in accordance with the main peaks of the XRD pattern of the representative iron scale (Fig. S1) [18]. The used chemicals and reagents are listed in Text S1.

2.2. Experimental processes

The experimental pipe reactor was custom-built to match the structural characteristics of the water supply pipe network (Fig. S2). Before the experiments, goethite was loaded onto the reactor. The experiments used tap water with stirring for 300 rpm, and the water quality parameters were summarized in Table S1. The analysis methods for water quality parameters were as described in Text S2. The initial concentrations of TCP and TBP were 2.0 $\mu\text{mol/L}$, while free chlorine (HClO/ClO^-) and goethite concentrations were 2.0 mg/L and 4.0 g/L, respectively. The temperature and pH were controlled at 7.5 ± 0.1 and 25 °C in the pipe reactor, which is close to the actual WDS conditions. Some parameters encompassed TCP/TBP concentrations (0.5 to 3.0 $\mu\text{mol/L}$), goethite dosages (2.0 to 8.0 g/L), pH values (6.5, 7.5, and 8.5) and HClO/ClO^- concentrations (0.5 to 3.0 mg/L) were chosen to assess the effects on TCP and TBP removal. Samples were collected periodically at predetermined time (0, 0.5, 1.0, 1.5, 2.0, 3.0, 4.0, 5.0, 6.0 and 8.0 min), filtered through a 0.22 μm microporous membrane, and quenched with freshly prepared sodium thiosulfate by adding 0.1 mL of $\text{Na}_2\text{S}_2\text{O}_3$ (the molar concentration was 1.0 mol/L).

To explore the impact of free radicals on TCP and TBP degradation, *tert*-butanol (TBA), benzoic acid (BA), and 1,4-dimethoxybenzene (DMOB) at a concentration of 150.0 $\mu\text{mol/L}$ were added to quench $\bullet\text{OH}$ and reactive chlorine species (RCS, chlorine radical ($\text{Cl}\bullet$) and

oxychloride radical ($\text{ClO}\bullet$)). The radicals competing experiments were performed by using TBA as a strong scavenger for $\bullet\text{OH}$, BA as a quenching agent for both $\bullet\text{OH}$ and $\text{Cl}\bullet$, and DMOB as a quenching agent for $\bullet\text{OH}$, $\text{Cl}\bullet$ and $\text{ClO}\bullet$. To analyze the intermediate products during the transformation, 30.0 mL samples were collected at a reaction of 1.0 h and quenched by 0.5 mL of $\text{Na}_2\text{S}_2\text{O}_3$. Then the samples were extracted to 2.0 mL using liquid/liquid extraction with *n*-hexane.

The instruments and methods used for analysis and characterization during the experimental process were displayed in Text S3.

3. Results and discussion

3.1. Goethite-mediated transformation of 2,4,6-trihalophenols

We hypothesized that goethite might influence the removal of organic compounds in water containing residual chlorine. To test this hypothesis, we firstly reacted TCP and TBP with goethite, a Fe-rich mineral, HClO/ClO^- , or both. Results show 19.2 % TCP removal with goethite alone and 27.2 % TCP removal using HClO/ClO^- alone after 8 min (Fig. 1a). For TBP, 22.5 % and 37.3 % were respectively removed in the same conditions (Fig. 1b). Removal increased to 60.8 % for TCP and 80.5 % for TBP using both goethite and chlorine, with corresponding rise of rate contents by 2.4–4.0 (Table S2). These findings suggested that goethite mediated chlorination enhanced the removal of aromatic phenolics. This might be explained either by transformation of aromatic phenolics into degradation products, or by adsorption of the initial compounds and degradation products on solid surfaces, such as goethite and flask surfaces.

High performance liquid chromatography-mass spectrometry (HPLC-MS) analysis revealed that the main products of TBP transformation with HClO/ClO^- were 4,6-dibromo-1,2-benzenediol (OP9-267.86), 2,6-dibromo-1,4-benzoquinone (OP12-265.84) and 3,5-dibromo-2-hydroxy-1,4-benzoquinone (OP13-281.84) (Table S3). 2-chloro-6-bromo-1,4-benzenediol (OP16-223.91), 2-bromo-6-chloro-1,4-benzoquinone (OP17-221.89) and 3-bromo-5-chloro-2-hydroxy-1,4-benzoquinone (OP18-235.89) were chlorine-containing intermediates. This suggests that the bromine atom on the phenol ring is substituted by chlorine during chlorination, according to previous studies [19]. In our study, the chlorine atom from free chlorine replaces the bromine atom at the ortho- or *para*-position of the phenol ring through electrophilic substitution. This is confirmed by the presence of 2,3,4,6-tetrachlorophenol (OP1-231.88) bearing 4 substituted chlorines atoms. No intermediate without aromatic ring could be found using HClO/ClO^- , suggesting that HClO/ClO^- does not possess sufficient energy to cleave the phenolic ring under our conditions.

By contrast, when both goethite and HClO/ClO^- were present, TCP degradation resulted in the formation of ring-cleavage compounds, including 2-chloro-4-oxohex-2-enedioic acid (OP4-194.00) and small molecular hexanedioic acid (OP5-160.04) (Table S4). Compared to the products from chlorination alone, the coexistence of goethite and HClO/ClO^- , resulted in the presence of ring-cleavage compounds during the reaction process, indicating the presence of stronger oxidants in the medium than HClO/OCl^- . Similar observations were made during the goethite mediated chlorination of TBP, thus strengthening this interpretation. Since the redox potential of hypochlorous acid (HClO/Cl^- , 0.89–1.48 V) is generally lower than that of $\bullet\text{OH}$ (2.80 V) [20], $\text{ClO}\bullet$ (1.49 V) [21], $\text{Cl}\bullet$ (1.50 V) [22], and $\text{Cl}_2\bullet^-$ (2.00 V) [21,23], we presumed that $\bullet\text{OH}$ could be the dominant species responsible for oxidation and ring opening, as suggested by a previous study [24]. The higher removal rates of TBP versus TCP is attributed to the lower C-Br bond energy in TBP (276 kJ/mol), versus that of the C-Cl bond in TCP (327 kJ/mol) [25].

3.2. Identification of active species

When goethite and HClO/ClO^- coexisted in aqueous media, a typical

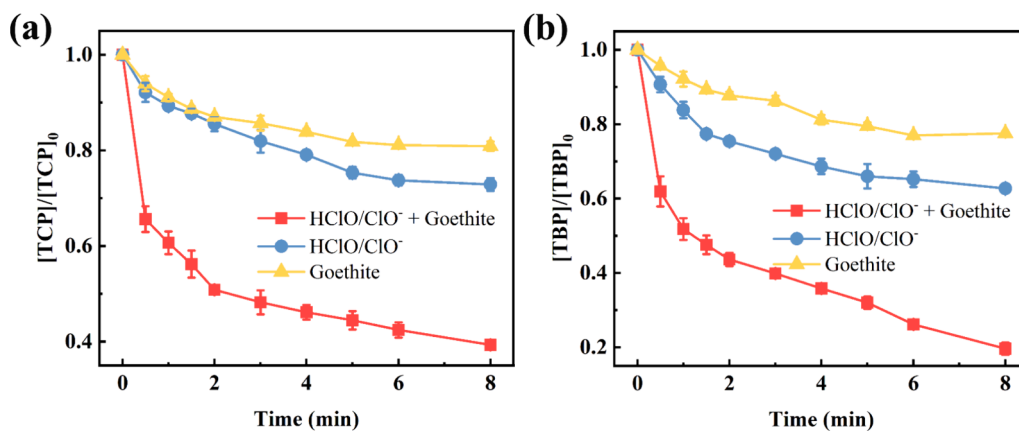
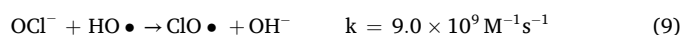
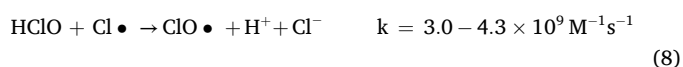
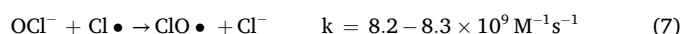
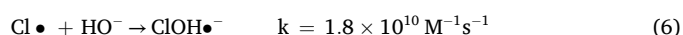
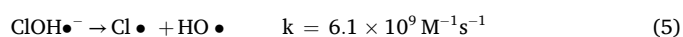
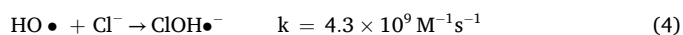
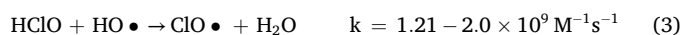
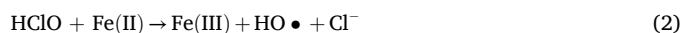
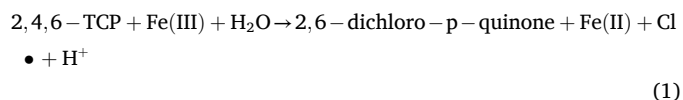


Fig. 1. The removal of (a) TCP and (b) TBP during the goethite mediated chlorination in batch-scale pipe reactor. (Experimental conditions: reaction time = 8.0 min, temperature = 25 ± 1 C, initial pH = 7.5 ± 0.1 , initial free chlorine = 2.0 mg/L, initial goethite dosage = 4.0 g/L, initial TCP and TBP concentration = 2.0 μ mol/L).

four-line EPR signal characteristic with relative intensity of 1:2:2:1 corresponding to a DMPO-OH spin adduct were observed (Fig. 2a). The three peaks located at 3494, 3509, and 3524 G were ascribed to DMPO-Cl, and the other six peaks indicated the production of DMPO-OCI [26,27]. The EPR capture experiment provided evidence that the active species (e.g., \bullet OH, $\text{ClO}\bullet$ and $\text{Cl}\bullet$) are responsible for the TCP/TBP removal.

According to the Haber-Weiss mechanism, dissolved and surface-exposed bivalent iron is a key reactant contributing to free radical generation. To exprobrated the effect of dissolved and surface-exposed bivalent iron, we attempted to determine the concentrations of Fe^{2+} and Fe^{3+} in water and goethite using ortho phenanthroline spectrophotometry (Text S4). However, no Fe^{2+} and Fe^{3+} could be detected above the detection limit of the method. Subsequently, when 50.0 μ g/L Fe^{2+} or 50.0 μ g/L Fe^{3+} was added separately to the HClO/ClO^- solution, it was found that the removal of TCP and TBP could be neglected (Fig. S3). Hence, the goethite dissolution had neglected effect to the TCP/TBP elimination in our experiments. To elucidate the surface chemical process of goethite, reaction of TCP with goethite was conducted in a separate experiment in Text S5. At the end of 24.0 h reaction, 15 % of TCP was removed from the aqueous solution. Nonetheless, no intermediates could be detected in the reaction solution. After washing the used goethite with methanol, the TCP and 2,6-dichloro-p-quinone leached out from the goethite and were obviously detected (Fig. S4) [28–30]. According to literature [31–34], we concluded that Fe(III) in goethite could function as an electrophilic oxidant able to oxidize TCP towards 2,6-dichloro-p-quinone, accompanied with the generation of Fe

(II) (Eq. (1)). Together with the EPR results above, Fe(II) in turn induced the formation of a series of free radicals (Eqs. 2–10) [15,21,35–37].



To further assess the effects of various free radicals, the removal situations of 2,4,6-trihalophenols during goethite mediated chlorination was investigated in conditions with added a series of scavengers. According to the reaction rates of each scavengers with free radicals

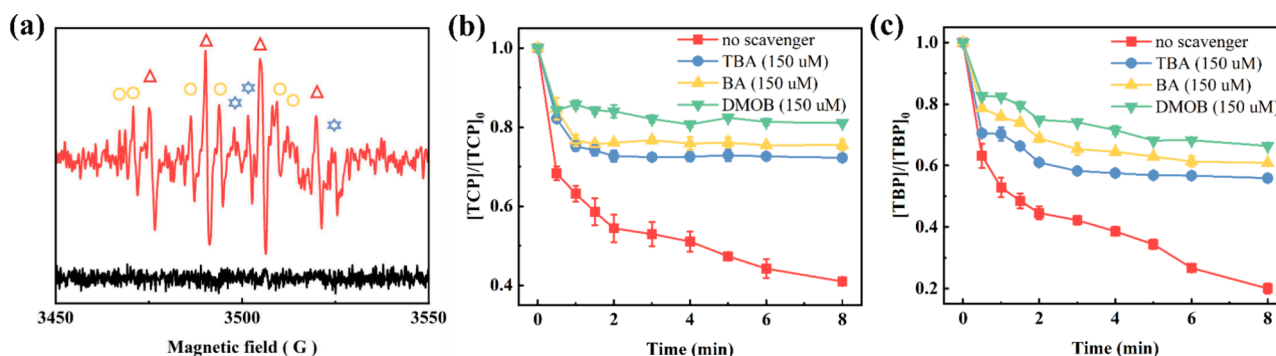


Fig. 2. (a) EPR spectra of DMPO adducts formed with radicals generated during the goethite mediated chlorination. Red triangles indicate the \bullet OH adduct; Blue hexagons indicate the $\text{Cl}\bullet$ adduct; and yellow circles indicate the $\text{ClO}\bullet$ adduct. The removal of (b) TCP and (c) TBP after addition of TBA, BA, and DMOB (150.0 μ M) during the goethite mediated chlorination in batch-scale pipe reactor. (Experimental conditions: Reaction time = 8.0 min, temperature = 25 ± 1 C, initial pH = 7.5 ± 0.1 , initial goethite dosage = 4.0 g/L, initial free chlorine concentration = 2.0 mg/L, initial TCP and TBP concentration = 2.0 μ mol/L). (For interpretation of the references to colour in this figure legend, the reader is referred to the web version of this article.)

(Table S5), TBA was preferred as the scavenger of $\cdot\text{OH}$ (reaction rate = $3.9 \times 10^9 \text{ M}^{-1} \text{ s}^{-1}$) [37], BA was selected as the scavenger of $\text{Cl}\cdot$ (reaction rate = $1.8 \times 10^{10} \text{ M}^{-1} \text{ s}^{-1}$) and $\cdot\text{OH}$ (reaction rate = $5.9 \times 10^9 \text{ M}^{-1} \text{ s}^{-1}$) [38,39], and DMOB was acted as a scavenger of $\cdot\text{OH}$ (reaction rate = $7.0 \times 10^9 \text{ M}^{-1} \text{ s}^{-1}$), $\text{Cl}\cdot$ (reaction rate = $1.8 \times 10^{10} \text{ M}^{-1} \text{ s}^{-1}$) and $\text{ClO}\cdot$ (reaction rate = $2.1 \times 10^9 \text{ M}^{-1} \text{ s}^{-1}$) [38,40]. As depicted in Fig. 2b and 2c, the addition of TBA resulted in a significant decrease in TCP and TBP removal, from 60.8 % to 27.8 % and from 80.5 % to 44.2 %, respectively. When BA and DMOB were introduced, TCP removal rates decreased to 24.6 % and 19.0 %, while TBP removal rates descended to 39.2 % and 33.6 %, respectively. To facilitate meaningful comparisons, we normalized the contribution rates of all active species to 100 %, as detailed in Table S6 and S7. This analysis elucidated that $\cdot\text{OH}$ predominantly influenced the removal rates of TCP and TBP, accounting for 87.44 % and 84.07 %, respectively (Fig. S5 and S6). This obviously inhibition effect implied that $\cdot\text{OH}$ was vital in the overall transformation of 2,4,6-trihalophenols. The relatively modest contribution of RCS was attributed to the fact that $\text{ClO}\cdot$ and $\text{Cl}\cdot$ had lower oxidation potential than that of $\cdot\text{OH}$, as mentioned above [23,41]. Overall, our findings revealed the major contribution of $\cdot\text{OH}$ in the transformation of 2,4,6-trihalophenols when goethite and HClO/ClO^- were present simultaneously.

3.3. Kinetics of surface reactions

In the heterogeneous catalytic reaction, either the Eley–Rideal model (where only TCP/TBP or free chlorine adsorbs on the goethite surface and reacts with other un-adsorbed substances) (eq (10) [42]) or the Langmuir–Hinshelwood model (where both reactants are adsorbed on the goethite surface and then react) (eq (11) [43,44]) is followed. The removal process of TCP/TBP was investigated through these two models.

$$k_{\text{app}} = \frac{K S k_{\text{TCP/TBP}}^n c_{\text{TCP/TBP}}^{n-1} (k_{\text{HClO/ClO}} - c_{\text{HClO/ClO}})^m}{(1 + (k_{\text{TCP/TBP}} c_{\text{TCP/TBP}})^n + (k_{\text{HClO/ClO}} - c_{\text{HClO/ClO}})^m)^2} \quad (10)$$

$$\frac{c_{\text{TCP/TBP}} c_{\text{HClO/ClO}}}{k_{\text{app}}} = \frac{1}{K} + \left(\frac{K_A}{K}\right) c_{\text{HClO/ClO}} \quad (11)$$

where K was the molar rate constant of goethite per square meter; S was the surface area of goethite normalized by the volume of the reaction solution; K_A represented the adsorption equilibrium coefficient; k_{TCP} , k_{TBP} , and $k_{\text{HClO/ClO}}$ represented the reaction coefficients of TCP, TBP and free chlorine (HClO/ClO^-), respectively; c_{TCP} , c_{TBP} and $c_{\text{HClO/ClO}}$ represented the concentrations of TCP, TBP and free chlorine (HClO/ClO^-), respectively. Based on previous research, the adsorption of TCP and TBP were most accurately represented by assuming an exponent of $n = 0.5$, while the adsorption of free chlorine followed a model with $m = 1$

[43,44].

The data of the L-H model and E-R model were shown in Fig. 3, Fig. S7 and Table S8. For the L-H model, the correlation coefficients (R^2) between TCP/TBP removal kinetics and different concentrations of TCP/TBP or free chlorine (HClO/ClO^-) were all greater than 0.99, which was far more than that of the E-R model ($R^2 < 0.75$). Thus, the reaction between aromatic DBPs and free chlorine (HClO/ClO^-) in the presence of goethite was more consistent with the L-H model. In other words, aromatic DBPs and free chlorine (HClO/ClO^-) were both adsorbed on the surface of goethite to undergo complex reactions.

The adsorption of reactants on the adsorbent surface is crucial for heterogeneous reactions, as the reaction rate highly relies on the adsorption of reactant molecules. Based on the L–H model, the values of k_{TCP} , k_{TBP} and $k_{\text{HClO/ClO}}$ are all around 10^4 , with little difference, indicating that TCP/TBP and free chlorine were both easy to be adsorbed on goethite surface. Hence, compared to the addition of goethite or HClO/ClO^- alone, aromatic DBPs and free chlorine (HClO/ClO^-) were adsorbed on the surface of goethite to increase the concentration of reactants, which accelerated the reaction rate of aromatic DBPs. According to previous literatures, the phenolic hydroxyl group could bond with the Fe (III) via H-bond [45], and the $-\text{OH}$ in TCP/TBP binding with Fe in goethite to form Fe–O–C [34].

On the basis of the above analysis, the goethite mediated chlorination in the WDS was a surface reaction, rather than the traditional view of homogeneous reaction. 2,4,6-trihalophenols and free chlorine (HClO/ClO^-) were both adsorbed on the surface of goethite. 2,4,6-trihalophenols reacted with HClO/ClO^- to produce electrons and hal-quinones. Fe(III)-goethite obtained electrons to form Fe(II)-goethite. Subsequently, HClO/ClO^- reacted with Fe(II)-goethite to form free radicals (e.g., $\cdot\text{OH}$, $\text{ClO}\cdot$, and $\text{Cl}\cdot$) via the Fenton-like reaction and oxidized Fe(II)-goethite to Fe(III)-goethite. Both free chlorine (HClO/ClO^-) and free radicals simultaneously reacted with 2,4,6-trihalophenols to form intermediates and aliphatic DBPs.

3.4. Effects of complex reaction conditions

Ensuring water quality in the distribution system is a key factor that guarantees public health. To further elucidate the influence of water environment, a heatmap was employed to visualize the impact of reaction conditions on the removal of 2,4,6-trihalophenol in the coexistence of goethite and free chlorine system (Fig. 4). The activation of free radicals was significantly enhanced with increasing concentrations of goethite and free chlorine, thus leading to improved removal of 2,4,6-trihalophenol.

In the real WDS, as the age of the pipe prolongs, the amounts of goethite tend to increase due to the corrosion around the internal surface of the pipe. The content of pipe-scale in aged pipes of WDS ranged from

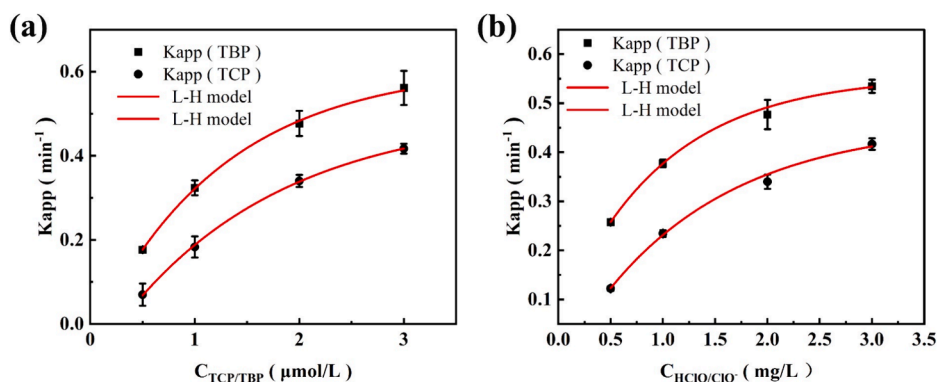


Fig. 3. L-H model fitting of different initial concentrations of (a) TCP and TBP and (b) free chlorine (HClO/ClO^-) on aromatic DBPs removal during the goethite mediated chlorination in batch-scale pipe reactor. (Experimental conditions: Reaction time = 8.0 min, temperature = $25 \pm 1^\circ\text{C}$, initial pH = 7.5 ± 0.1 , initial goethite dosage = 4.0 g/L).

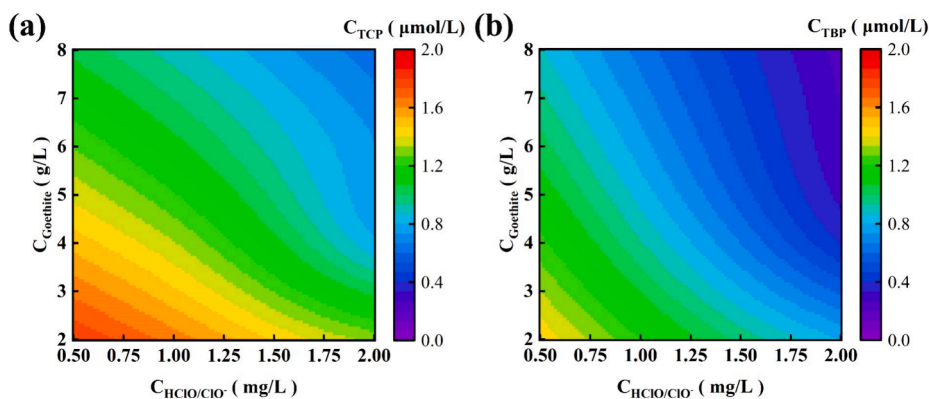


Fig. 4. The heatmap of the effect of free chlorine concentrations and goethite doses on the degradation of TCP (a) and TBP (b) during the goethite-mediated chlorination in batch-scale pipe reactor. (Experimental conditions: Reaction time = 8.0 min, temperature = 25 ± 1 C, initial pH = 7.5 ± 0.1 , initial TCP and TBP concentration = 2.0 $\mu\text{mol/L}$).

0.2 to 8.0 g/L [46,47]. As shown in Fig. S8, when goethite varied from 2.0 to 8.0 g/L, the decay of TCP and TBP was enhanced 2.0-fold and 1.5-fold, respectively. Considering the presence of magnetite in corrosion pipe scale, we have included experiments involving magnetite in our study. We observed that as the ratio of goethite to magnetite increased, the removal of 2,4,6-trihalophenols also increased accordingly (Fig. S9). Because the irregular surface and pores of goethite typically offers more active sites for the formation of $\cdot\text{OH}$ radical, potentially leading to faster degradation of pollutants [48]. Therefore, from the viewpoint of hydroxyl radical process induced by goethite, the presence of scale accelerates the transformation of aromatic disinfection byproducts.

Given the fact of the residual chlorine (HClO/ClO^-) remaining from 0.05 to 2.0 mg/L in WDS, we investigated the TCP/TBP conversion as a function of HClO/ClO^- . The gradual increase in TCP/TBP removal efficiency is evident with the increasing concentration of HClO/ClO^- , as demonstrated in Fig. S10. This enhancement was expected since higher residual chlorine (HClO/ClO^-) concentrations facilitated the formation of active species for the effective degradation of TCP/TBP (Eq. (3)). The results indicated that the destruction of aromatic components mainly occurred in the initial stage of WDS because the chlorine (HClO/ClO^-) concentration usually decays while the water flows through pipelines [49]. In addition, pH value is an important factor affecting aromatic DBPs transformation in the WDS. As evidenced above, degradation of TCP/PBP followed L-H model, indicating that the significance of organic compound and HClO adsorption on the goethite surface. As displayed in Fig. S10, weak alkaline condition is not conducive to TCP/TBP conversion. At pH higher than 7.5, the surface of the goethite bears a negative charge [50–52] due to its p H_{pzc} of 6.99 [53]. Free chlorine at the pH above 8.0 tends to exist in the major form of OCl^- [54,55]. Moreover, TCP^- and TBP^- are present in negatively ionized form rather than molecular form as a consequence of p K_a 5.99 for TCP and 5.94 for TBP, respectively [56,57]. Thus, weak alkaline condition in the WDS is unfavorable to the adsorption of both free chlorine and halogenated phenol via electrostatic attraction. The conversion of phenolic pollutants is inhibited accordingly.

3.5. Degradation products

The major intermediates of TCP and TBP treated with the goethite mediated chlorination were identified (Fig. S12–17). The DFT calculation was used to validate the degradation pathways. According to the frontier molecular orbital theory, the highest occupied molecular orbital (HOMO), the lowest unoccupied molecular orbital (LUMO), and the corresponding related energies were calculated. Atoms with higher values of $\text{FED}_{\text{HOMO}}^2 + \text{FED}_{\text{LUMO}}^2$ were easily attacked by free radicals to undergo hydroxyl substitution reactions (Fig. S18 and Table S9) [58,59].

Based on the identified intermediates and theoretical calculations, the $2\text{FED}_{\text{HOMO}}^2$ of C(1), C(2), C(3), C(4), C(6) on the benzene ring were relatively high, hence, three reaction pathways on TCP transformation were proposed (Fig. 5a). On pathway I, within the bulk containing chloride ions, a potential reaction occurs between ClO^-/Cl^- and 2,4,6-TCP, resulting in the formation of OP1-231.88 [7]. On pathway II, the reaction mechanism of 2,4,6-TCP is influenced by the selective elimination of Cl from the ortho- or para- positions, followed by the attack of $\cdot\text{OH}$ radical, ultimately leading to the formation of OP2-177.96 [60]. Furthermore, the fragments were degraded into OP3-159.99 through the attack of $\cdot\text{OH}$ and removal of Cl atom. Due to the low bond energy of C-Cl [61], electrophilic substitution reactions were easy to be occurred in C-Cl under the attack of $\cdot\text{OH}$ [62,63]. The presence of three hydroxyl groups in the phenol activated the ring, and hence, facilitating the ring cleavage process. Since OP3-159.99 had a strong negative potential region, OP4-194.00 and OP5-160.04 were produced from the cleavage of the benzene ring [64]. In particular, the open-chain compounds were only detected in goethite mediated chlorination but not in the chlorination-only process. It was deduced that the ring cleavage was attributed to the radical mediated reaction [65–67].

On pathway III, the C(4) attached to the phenolic hydroxyl group on TCP underwent a one-electron oxidation step with the attack of $\cdot\text{OH}$, resulting in the formation of a carbon-centered radical [68–70]. Through a subsequent one-electron oxidation step under the attack of radicals, 2,4,6-TCP could be transformed into the carbon-centered radical cation, leading to the generation of OP6-175.94 following deprotonation and elimination of HCl [7]. Additionally, it is observed that free radicals preferentially target the para- and ortho-positions of the phenolic hydroxyl [60]. Two sub-pathways were derived from OP6-175.94, one of which involved the reaction between OP6-175.94 and $\cdot\text{OH}$ (formed during the goethite mediated redox reaction between Fe (II)-goethite and HClO/ClO^-) to form OP7-191.94 [71]. And the other sub-pathway was formation of OP2-177.96 and OP8-161.96 via hydrolysis, addition and elimination reaction [7].

The transformation pathway of TBP degradation during the goethite-mediated chlorination was proposed in Fig. 5b. According to the DFT analysis, the C(6), C(7), C(10) site connecting bromine on the TBP structure presented a higher value of $\text{FED}_{\text{HOMO}}^2 + \text{FED}_{\text{LUMO}}^2$, which was more vulnerable for free radical attack. TBP transformation also had three possible pathways. The pathway I and II were similar to the TCP conversion pathways. In stark contrast, on pathway III, the three bromine atoms in the benzene ring were seem to be easily replaced by chlorine to generate bromochlorophenol because of the high electron cloud density [19]. In the presence of $\cdot\text{OH}$, the Cl on OP15-241.87 was attacked and replaced by $\cdot\text{OH}$, leading to the conversion of OP15-241.87 into OP16-223.91, and then further transformed to OP17-221.89 and OP18-235.892. Compared with TCP transformation, TBP reacted with

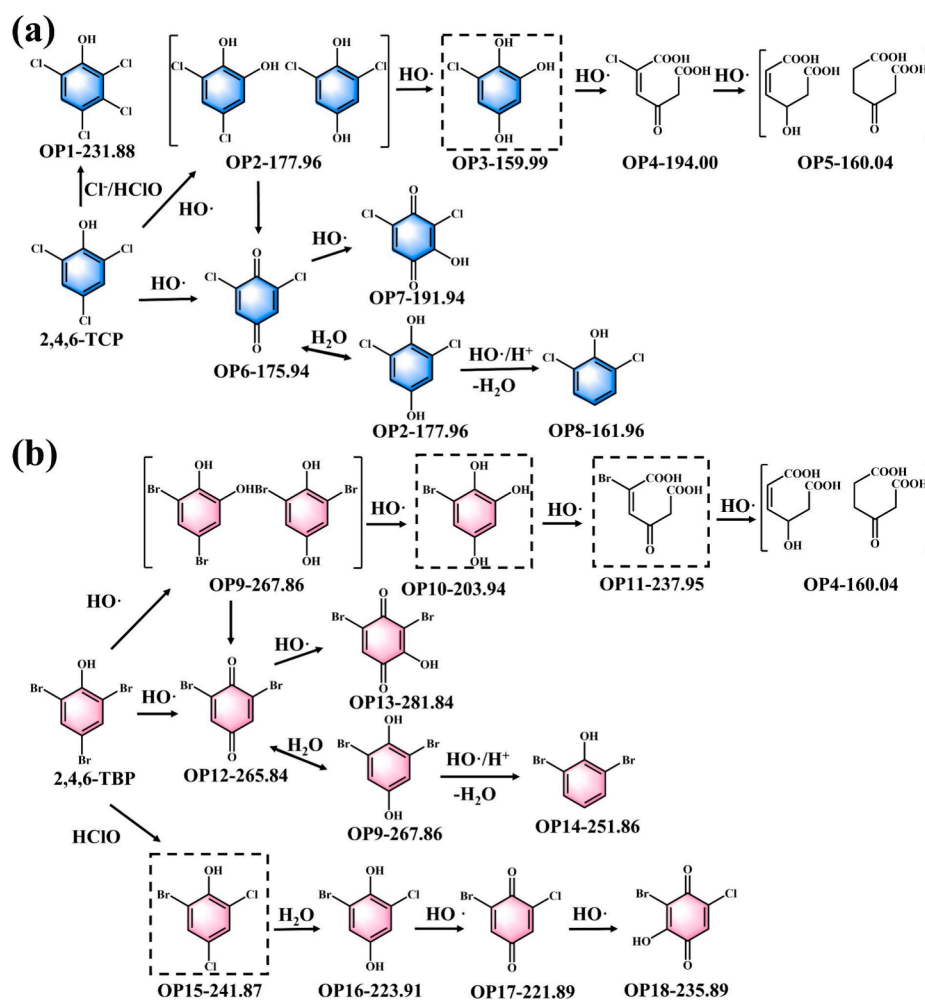


Fig. 5. The proposed pathways of (a) TCP and (b) TBP during the goethite mediated chlorination in batch-scale pipe reactor. (Experimental conditions: Reaction time = 1.0 h, temperature = 25 ± 1°C, initial pH = 7.5 ± 0.1, initial goethite dosage = 4.0 g/L, initial free chlorine concentration = 2.0 mg/L, initial TCP and TBP concentration = 2.0 μmol/L).

chlorine-containing disinfectants to generate chlorinated aromatic DBPs and brominated aromatic DBPs. Furthermore, the intermediate products were also analyzed by adding TBA (Fig. S19 and S20). During the reaction, only chlorine-substituted products were detected, and hydroxyl radical oxidation products and ring-opening products were not detected. Therefore, free radicals triggered by goethite mediated chlorination exhibited greater efficacy in ring cleavage for the complete degradation

of TCP and TBP compared to chlorination alone.

3.6. Formation of aliphatic DBPs during goethite-mediated chlorination

The concentrations of aliphatic DBP formation were further confirmed in the transformation of aromatic DBPs, including four trihalomethanes (THMs, chloroform (TCM), tribromomethane (TBM),

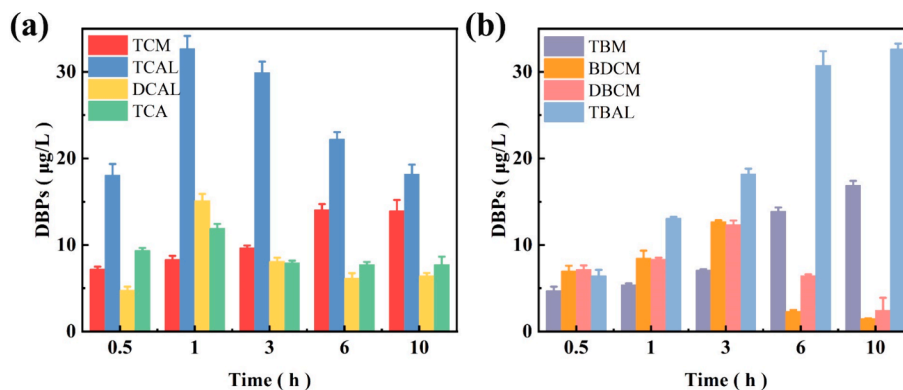


Fig. 6. The formation of trihalomethanes (THMs), haloacetaldehyde (HALs) and trichloroacetone (TCA) from (a) TCP and (b) TBP during the goethite mediated chlorination in batch-scale pipe reactor. (Experimental conditions Reaction time = 10.0 h, temperature = 25 ± 1°C, initial pH = 7.5 ± 0.1, initial goethite dosage = 4.0 g/L, initial free chlorine concentration = 2.0 mg/L, initial TCP and TBP concentration = 2.0 μmol/L).

bromodichloromethane (BDCM), and chlorodibromomethane (DBCM)), three haloacetaldehyde (HALS, trichloroacetaldehyde (TCAL), dichloroacetaldehyde (DCAL), and tribromoacetaldehyde (TBAL)) and trichloroacetone (TCA).

Fig. 6a illustrates that TCM, TCAL, DCAL and TCA were the main byproducts during the chlorination of TCP. The concentration of THMs kept increasing over time in the chlorination of TCP, supporting the assumption that the transformation products such as ring-cleavage compounds (OP4-194.00) and small molecular hexanedioic acid (OP5-160.04) acted as intermediates and further decomposed to form aliphatic halogenated DBPs. The formation of TCAL initially increased to 27.7 $\mu\text{g/L}$ and then decreased to 17.9 $\mu\text{g/L}$ during the reaction. The trends of DCAL and TCA formation were similar with TCAL. Due to sufficient free chlorine at the beginning of the reaction, TCP was rapidly degraded to form aliphatic DBPs. After 1 h of reaction, the decrease of free chlorine and TCP resulted the lower formation rate of TCA and HALS than that of conversion rate. Moreover, the change in TCAL and DCAL concentration may be related to α , β -unsaturated C4-dialdehydes [72]. Several current studies have reported the formation of α , β -unsaturated C4-dialdehydes as more toxic DBPs during chlorination of TCP [73]. Based on the detection of ring-opening products and haloacetaldehyde (e.g., TCAL and DCAL) during the reaction process, we infer the potential formation of α , β -unsaturated C4-dialdehydes during goethite-mediated chlorination. Fig. 6b shows the formation of TBM, BDCM,

DBCM, and TBAL during the conversion of TBP. TBM and TBAL exhibited a gradual increase over the course of the reaction, while BDCM and DBCM displayed an initial increase followed by a decrease. After stopping the reaction, TBM and TBAL emerged as the predominant DBPs, constituting 31.6 % and 61.1 % respectively. Previous research has suggested that BDCM and DBCM could be oxidized and converted into TBM and TBAL in the presence of free chlorine [48].

3.7. Cytotoxicity assay during transformation of aromatic DBPs

TCP and TBP were transformed to form some intermediates and aliphatic DBPs during the goethite mediated $\cdot\text{OH}$ oxidation, it is essential to assess the toxicity of the reaction system. As shown in Fig. 7a and 7c, the relative viability of CHO cells exposed to TCP and TBP in chlorination alone and goethite mediated chlorination was compared. The relative viability of TCP and TBP in chlorination alone (97.75 % and 95.76 %) was approximately 1.28 and 1.21 times higher than that in goethite mediated chlorination (76.47 % and 79.35 %), respectively. Since TCP could produce more toxic α , β -unsaturated C4-dialdehydes during chlorination alone, these α , β -unsaturated C4-dialdehydes could be further oxidized by free radicals in the goethite mediated chlorination process, thus reducing the toxicity of TCP in the goethite system [72,73]. Thus, the transformation process of aromatic DBPs in the presence of residual chlorine and goethite was beneficial to weaken

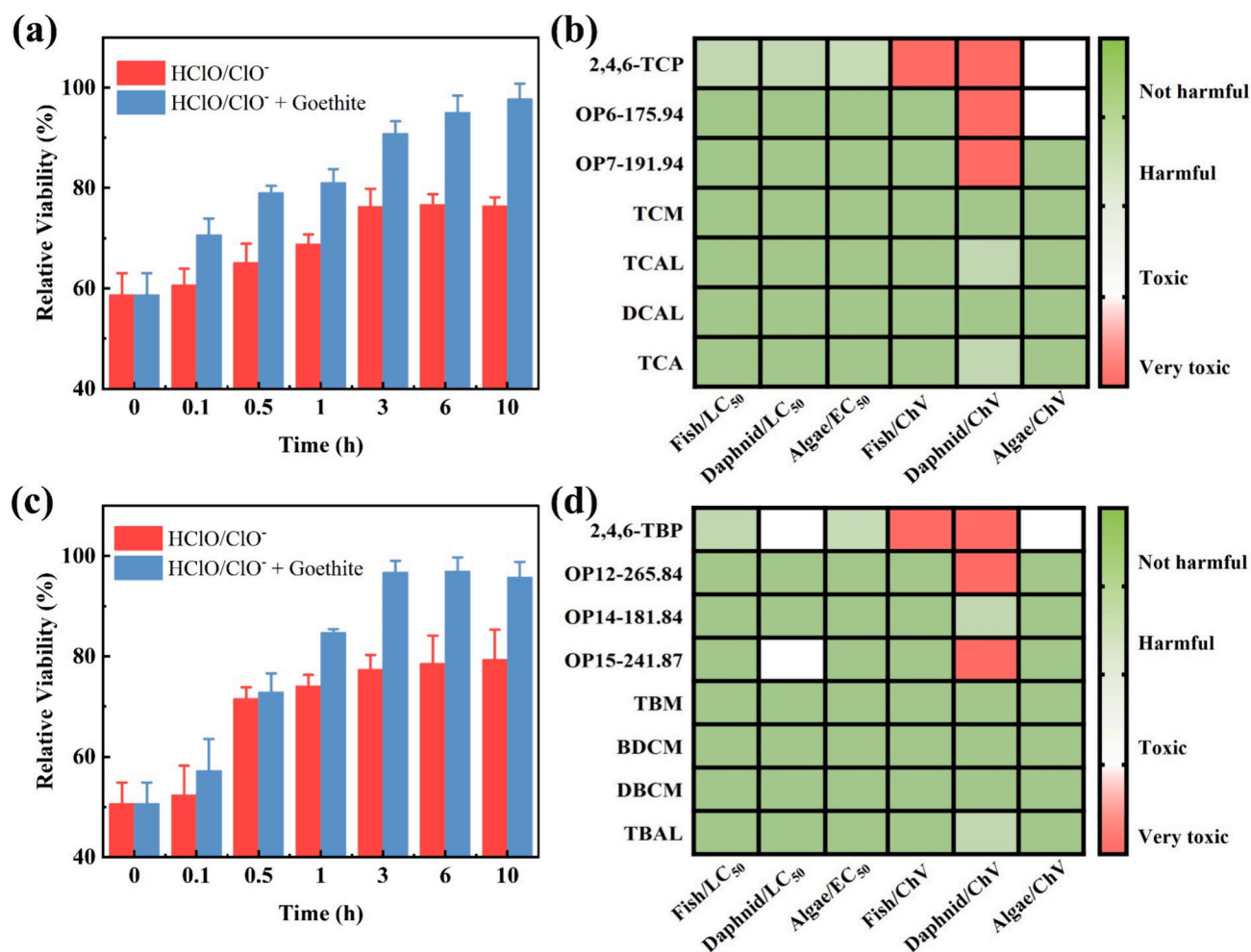


Fig. 7. The relative viability of CHO cells exposed to (a) TCP and (c) TBP in different reaction systems at different reaction times during the goethite mediated chlorination in batch-scale pipe reactor; predicting the acute/chronic toxicity of various intermediates of (b) TCP and (d) TBP to fish, daphnia, and green algae using ECOSAR software. (Experimental conditions: Reaction time = 10.0 h, temperature = 25 \pm 1C, initial pH = 7.5 \pm 0.1, initial goethite dosage = 4.0 g/L, initial free chlorine concentration = 2.0 mg/L, initial TCP and TBP concentration = 2.0 $\mu\text{mol/L}$.) (For interpretation of the references to colour in this figure legend, the reader is referred to the web version of this article.)

the toxicity of water quality. According to toxicity software calculations (Fig. 7b and 7d and Table S10), the toxicity of aliphatic compounds (such as trihalomethanes, haloacetaldehyde, and trichloroacetone) was found to be lower than that of 2,4,6-trihalophenol and aromatic intermediates. The previous researches have certified that halogenated compounds with aromatic ring exhibited higher toxicity than aliphatic compounds [74,75]. The potential contribution of the aromatic ring was contributed to the higher toxicity of 2,4,6-trihalophenols. Furthermore, some of the ring-opened products were also toxic, which was related to the unsaturated C-C or C-O double bonds [76]. When aromatic structures were gradually transformed into aliphatic structures by hydroxyl radicals, the toxicity of 2,4,6-trihalophenols-containing water decreases accordingly. Therefore, hydroxyl radical with high oxidation capacity produced in goethite mediated chlorination system contributed to the effective detoxification of organo chlorine pollutants.

4. Conclusions

In conclusion, this research focused on the decomposition of 2,4,6-trihalophenols (e.g., TCP and TBP) by the interface free radicals triggered by goethite mediated chlorination. It was found that various free radicals (e.g., $\cdot\text{OH}$, $\text{ClO}\cdot$ and $\text{Cl}\cdot$) were generated by transferring electrons from 2,4,6-trihalophenols to goethite for activating residual chlorine. The $\cdot\text{OH}$ served as dominant active species responsible for organic compounds degradation. Higher concentrations of goethite and free chlorine promoted the decomposing of 2,4,6-trihalophenols, and the process followed the L-H model. The degradation process involved ring opening, oxidation, substitution, addition, hydrolysis, accompanied by effective detoxification. Notably, in contrast to the traditional negative understanding of pipe scales on DBP formation and transformation, we proposed a positive effect of free radical process induced by goethite. This work reveals novel insights into the risk assessment of pipe scale in the WDS.

CRedit authorship contribution statement

Feilong Dong: Writing – original draft, Funding acquisition, Formal analysis, Data curation, Conceptualization. **Jiani Zhu:** Writing – original draft, Methodology, Formal analysis, Data curation. **Cong Li:** Writing – review & editing, Methodology. **Eric Lichtfouse:** . **Wei Wang:** Writing – review & editing, Project administration, Conceptualization. **Shuang Song:** Writing – review & editing, Project administration, Formal analysis, Conceptualization.

Declaration of competing interest

The authors declare that they have no known competing financial interests or personal relationships that could have appeared to influence the work reported in this paper.

Data availability

Data will be made available on request.

Acknowledgments

This work was financially supported by the National Natural Science Foundation of China (No. 52100015), the Zhejiang Provincial Natural Science Foundation of China (Grants LQ22E080018) and the China Postdoctoral Science Foundation (2021M692860).

Appendix A. Supplementary data

Supplementary data to this article can be found online at <https://doi.org/10.1016/j.cej.2024.152390>.

References

- [1] T.A. Bellar, J.J. Lichtenberg, R.C. Kroner, The occurrence of organohalides in chlorinated drinking waters, *J. Am. Water Works Assoc.* 66 (12) (1974) 703–706.
- [2] X. Liu, L. Chen, M. Yang, C. Tan, W. Chu, The occurrence, characteristics, transformation and control of aromatic disinfection by-products: A review, *Water Res.* 184 (2020) 116076.
- [3] X. Jiang, P. Shi, L. Jiang, J. Qiu, B. Xu, Y. Pan, Q. Zhou, In vivo toxicity evaluations of halophenolic disinfection byproducts in drinking water: A multi-omics analysis of toxic mechanisms, *Water Res.* 218 (2022) 118431.
- [4] Z. Zhang, Q. Zhu, C. Huang, M. Yang, J. Li, Y. Chen, B. Yang, X. Zhao, Comparative cytotoxicity of halogenated aromatic DBPs and implications of the corresponding developed QSAR model to toxicity mechanisms of those DBPs: Binding interactions between aromatic DBPs and catalase play an important role, *Water Res.* 170 (2020) 115283.
- [5] S. Karlsson, S. Kaugare, A. Grimvall, H. Boren, R. Savenhed, Formation of 2,4,6-trichlorophenol and 2,4,6-trichloroanisole during treatment and distribution of drinking water, *Water Sci. Technol.* 31 (11) (1995) 99–103.
- [6] Y. Li, Y. Li, B. Jin, K. Zhang, L. Wang, J. Zhao, Effects of 2,4,6-trichlorophenol and its intermediates on acute toxicity of sludge from wastewater treatment and functional gene expression, *Bioresour. Technol.* 323 (2021) 124627.
- [7] R. Xu, H. Ren, T. Chi, Y. Zheng, Y. Xie, J. Tian, L. Chen, Ozone oxidation of 2,4,6-TCP in the presence of halide ions: Kinetics, degradation pathways and toxicity evaluation, *Chemosphere* 288 (2) (2022) 132343.
- [8] Q. Xia, X. Zhang, Manual on water quality standards, China Environ. Sci. Press, Beijing, China, 1990.
- [9] P. Sarin, V.L. Snoeyink, J. Bebee, W.M. Kriven, J.A. Clement, Physico-chemical characteristics of corrosion scales in old iron pipes, *Water Res.* 35 (2001) 2961–2969.
- [10] Z. Niu, Y. Wang, X. Zhang, W. He, H. Han, P. Yin, Iron stability in drinking water distribution systems in a city of China, *J. Environ. Sci.* 18 (1) (2006) 40–46.
- [11] Z. Mi, X. Zhang, C. Chen, Iron release in drinking water distribution systems by feeding desalinated seawater: characteristics and control, *Des. Water Treat.* 57 (21) (2016) 9728–9735.
- [12] J. Bandara, J.A. Mielczarski, J.I. Kiwi, Adsorption mechanism of chlorophenols on iron oxides, titanium oxide and aluminum oxide as detected by infrared spectroscopy, *Appl. Cat. B* 34 (4) (2001) 307–320.
- [13] J. Wu, J. Zhao, J. Hou, B. Xing, The fate of p-nitrophenol in goethite-rich and sulfide-containing dynamic anoxic/oxic environments, *Environ. Sci. Tech.* 54 (15) (2020) 9427–9436.
- [14] C. Hu, J. Zhang, B. Xu, Y. Lin, T. Zhang, F. Tian, Effect of pipe corrosion product goethite on the formation of disinfection by-products during chlorination, *Desalination and Water Treat.* 57 (2) (2014) 553–561.
- [15] F.Z. Meghlaoui, S. Merouani, O. Hamdaoui, M. Bouhelassa, M. Ashokkumar, Rapid catalytic degradation of refractory textile dyes in Fe (II)/chlorine system at near neutral pH: radical mechanism involving chlorine radical anion ($\text{Cl}_2\cdot^-$)-mediated transformation pathways and impact of environmental matrices, *Sep. Purif. Technol.* 227 (2019) 115685.
- [16] Y. Zong, X. Guan, J. Xu, Y. Feng, Y. Mao, L. Xu, H. Chu, D. Wu, Unraveling the overlooked involvement of high-valent cobalt-oxo species generated from the cobalt (II)-activated peroxymonosulfate process, *Environ. Sci. Tech.* 54 (24) (2020) 16231–16239.
- [17] X. Li, W.A. Mitch, Drinking water disinfection byproducts (DBPs) and human health effects: multidisciplinary challenges and opportunities, *Environ. Sci. Tech.* 52 (4) (2018) 1681–1689.
- [18] H. Wang, C. Hu, X. Hu, M. Yang, J. Qu, Effects of disinfectant and biofilm on the corrosion of cast iron pipes in a reclaimed water distribution system, *Water Res.* 46 (4) (2012) 1070–1078.
- [19] H. Zhai, X. Zhang, Formation and decomposition of new and unknown polar brominated disinfection byproducts during chlorination, *Environ. Sci. Tech.* 45 (6) (2011) 2194–2201.
- [20] L. Wang, X. Yuan, H. Zhong, H. Wang, Z. Wu, X. Chen, G. Zeng, Release behavior of heavy metals during treatment of dredged sediment by microwave-assisted hydrogen peroxide oxidation, *Chem. Eng. J.* 258 (2014) 334–340.
- [21] J. Fang, Y. Fu, C. Shang, The roles of reactive species in micropollutant degradation in the UV/free chlorine system, *Environ. Sci. Tech.* 48 (3) (2014) 1859–1868.
- [22] P. Neta, R.E. Huie, A.B. Ross, Rate constants for reactions of inorganic radicals in aqueous solution, *J. Phys. Chem. Ref. Data* 17 (3) (1988) 1027–1284.
- [23] C. McBride, The Investigation of the Chemical Degradation of the Acetate Ion under Operating Conditions Relevant to Pressurised Water Reactors, University of Manchester, 2022.
- [24] H. Ji, F. Chang, X. Hu, W. Qin, J. Shen, Photocatalytic degradation of 2,4,6-trichlorophenol over g-C₃N₄ under visible light irradiation, *Chem. Eng. J.* 218 (2013) 183–190.
- [25] K.D. Bobyk, D.P. Ballou, S.E. Rokita, Rapid kinetics of dehalogenation promoted by iodotyrosine deiodinase from human thyroid, *Biochem.* 54 (29) (2015) 4487–4494.
- [26] Q. Wang, T. Li, C. Yang, M. Chen, A. Guan, L. Yang, S. Li, X. Lv, Y. Wang, G. Zheng, Electrocatalytic methane oxidation greatly promoted by chlorine intermediates, *Angew. Chem. Int. Ed.* 60 (32) (2021) 17398–17403.
- [27] H. Li, J. Li, Z. Ai, F. Jia, L. Zhang, Oxygen vacancy-mediated photocatalysis of BiOCl: reactivity, selectivity, and perspectives, *Angew. Chem. Int. Ed.* 57 (1) (2018) 122–138.
- [28] C. Tai, J. She, Y. Yin, T. Zhao, L. Wu, Degradation of 2,4,6-Trichlorophenol Using Hydrogen Peroxide Catalyzed by Nanoscale Zero-Valent Iron Supported on Ion Exchange Resin, *J. Nanosci. Nanotechnol.* 16 (6) (2016) 5850–5855.

- [29] C. Han, Y. Ye, G. Wang, W. Hong, C. Feng, Selective electro-oxidation of phenol to benzoquinone/hydroquinone on polyaniline enhances capacitance and cycling stability of polyaniline electrodes, *Chem. Eng. J.* 347 (2018) 648–659.
- [30] C. Chen, Y. Wang, Y. Huang, J. Hua, W. Qu, D. Xia, C. He, V.K. Sharma, D. Shu, Overlooked self-catalytic mechanism in phenolic moiety-mediated Fenton-like system: Formation of Fe(III) hydroperoxide complex and co-treatment of refractory pollutants, *Appl. Catal., B* 321 (2023).
- [31] X. Zhao, Y. Li, J. Wang, Z. Ouyang, J. Li, G. Wei, Z. Su, Interactive oxidation-reduction reaction for the in situ synthesis of graphene-phenol formaldehyde composites with enhanced properties, *Appl. Mater. Interfaces* 6 (6) (2014) 4254–4263.
- [32] X. Xu, R. Xiao, D.D. Dionysiou, R. Spinney, T. Fu, Q. Li, Z. Wang, D. Wang, Z. Wei, Kinetics and mechanisms of the formation of chlorinated and oxygenated polycyclic aromatic hydrocarbons during chlorination, *Chem. Eng. J.* 351 (2018) 248–257.
- [33] A. Sorokin, S. De Suzzoni-Dezard, D. Poullain, J.P. Noël, B. Meunier, CO₂ as the ultimate degradation product in the H₂O₂ oxidation of 2,4,6-trichlorophenol catalyzed by iron tetrasulfophthalocyanine, *J. Am. Chem. Soc.* 118 (31) (1996) 7410–7411.
- [34] F.J. Rivas, F.J. Beltrán, J.F. Garcia-araya, V. Navarrete, O. Gimeno, Co-oxidation of p-hydroxybenzoic acid and atrazine by the Fenton's like system Fe(III)/H₂O₂, *J. Hazard. Mater.* 91 (1–3) (2002) 143–157.
- [35] T. Zhu, J. Deng, S. Zhu, A. Cai, C. Ye, X. Ling, H. Guo, Q. Wang, X. Li, Kinetic and mechanism insights into the degradation of venlafaxine by UV/chlorine process: A modelling study, *Chem. Eng. J.* 431 (2022).
- [36] H. Zhang, Y. Liu, L. Wang, Z. Li, X. Lu, T. Yang, J. Ma, Enhanced Radical Generation in an Ultraviolet/Chlorine System through the Addition of TiO₂, *Environ. Sci. Tech.* 55 (17) (2021) 11612–11623.
- [37] K. Guo, Z. Wu, C. Shang, B. Yao, S. Hou, X. Yang, W. Song, J. Fang, Radical Chemistry and Structural Relationships of PPCP Degradation by UV/Chlorine Treatment in Simulated Drinking Water, *Environ. Sci. Tech.* 51 (18) (2017) 10431–10439.
- [38] P. Wang, L. Bu, Y. Wu, J. Deng, S. Zhou, Mechanistic insights into paracetamol transformation in UV/NH₂Cl process: Experimental and theoretical study, *Water Res.* 194 (2021) 116938.
- [39] P. Sun, T. Meng, Z. Wang, R. Zhang, H. Yao, Y. Yang, L. Zhao, Degradation of Organic Micropollutants in UV/NH₂Cl Advanced Oxidation Process, *Environ. Sci. Tech.* 53 (15) (2019) 9024–9033.
- [40] J.E. Grebel, J.J. Pignatello, W.A. Mitch, Effect of halide ions and carbonates on organic contaminant degradation by hydroxyl radical-based advanced oxidation processes in saline waters, *Environ. Sci. Tech.* 44 (2010) 6822–6828.
- [41] L. Huang, T. Zeng, X. Xu, Z. He, J. Chen, S. Song, Immobilized hybrids between nitrogen-doped carbon and stainless steel derived Fe₃O₄ used as a heterogeneous activator of persulfate during the treatment of aqueous carbamazepine, *Chem. Eng. J.* 372 (2019) 862–872.
- [42] A. Mulay, V.K. Rathod, Microwave-assisted heterogeneous esterification of dibutyl maleate: Optimization using response surface methodology, *Chem. Data Collect.* 34 (2021).
- [43] S. Wunder, Y. Lu, M. Albrecht, M. Ballauff, Catalytic Activity of Faceted Gold Nanoparticles Studied by a Model Reaction: Evidence for Substrate-Induced Surface Restructuring, *ACS Catal.* 1 (8) (2011) 908–916.
- [44] L. Huang, H. Zhang, T. Zeng, J. Chen, S. Song, Synergistically enhanced heterogeneous activation of persulfate for aqueous carbamazepine degradation using Fe₃O₄@SBA-15, *Sci. Total Environ.* 760 (2021) 144027.
- [45] Y. Zhuang, B. Han, R. Chen, B. Shi, Mechanism study on organic pollutant accumulation by iron-based particles in drinking water conditions, *Chem. Eng. J.* 396 (1) (2020) 125157.
- [46] J. Liu, H. Chen, L. Yao, Z. Wei, L. Lou, Y. Shan, S. Endalkachew, N. Mallikarjuna, B. L. Hu, X.Y. Zhou, The spatial distribution of pollutants in pipe-scale of large-diameter pipelines in a drinking water distribution system, *J. Hazard. Mater.* 317 (2016) 27–35.
- [47] J. Liu, H. Chen, Q. Huang, L. Lou, B. Hu, S.D. Endalkachew, N. Mallikarjuna, Y. Shan, X. Zhou, Characteristics of pipe-scale in the pipes of an urban drinking water distribution system in eastern China, *Water Sci. Technol. Water Supply* 16 (3) (2016) 715–726.
- [48] L. Zhao, Z. Lin, X. Ma, Catalytic activity of different iron oxides: Insight from pollutant degradation and hydroxyl radical formation in heterogeneous Fenton-like systems, *Chem. Eng. J.* 352 (2018) 343–351.
- [49] F. García-Ávila, A. Avilés-Añazco, J. Ordoñez-Jara, C. Guanuchi-Quezada, L. Flores del Pino, L. Ramos-Fernández, Modeling of residual chlorine in a drinking water network in times of pandemic of the SARS-CoV-2 (COVID-19), *Sustainable, Environ. Res.* 31 (2021) 1–15.
- [50] T. Zhang, C. Li, J. Ma, H. Tian, Z. Qiang, Surface hydroxyl groups of synthetic α-FeOOH in promoting •OH generation from aqueous ozone: Property and activity relationship, *Appl Catal B* 82 (1–2) (2008) 131–137.
- [51] H. Zhang, H. Fu, D. Zhang, Degradation of C.I. Acid Orange 7 by ultrasound enhanced heterogeneous Fenton-like process, *J. Hazard. Mater.* 172 (2–3) (2009) 654–660.
- [52] J. Park, H. Choi, J. Cho, Kinetic decomposition of ozone and para-chlorobenzoic acid (pCBA) during catalytic ozonation, *Water Res.* 38 (9) (2004) 2284–2291.
- [53] Y. Zhao, F. Liu, X. Qin, Adsorption of diclofenac onto goethite: Adsorption kinetics and effects of pH, *Chemosphere* 180 (2017) 373–378.
- [54] S. Subhan, A. Ur Rahman, M. Yaseen, H. Ur Rashid, M. Ishaq, M. Sahibzada, Z. Tong, Ultra-fast and highly efficient catalytic oxidative desulfurization of dibenzothiophene at ambient temperature over low Mn loaded Co-Mo/Al₂O₃ and Ni-Mo/Al₂O₃ catalysts using NaClO as oxidant, *Fuel* 237 (2019) 793–805.
- [55] W. Li, E. Cho, Coal Desulfurization with Sodium Hypochlorite, *Energy Fuels* 19 (2005) 499–507.
- [56] J. Li, X. Long, H. Yin, J. Qiao, H. Lian, Magnetic solid-phase extraction based on a polydopamine-coated Fe₃O₄ nanoparticles absorbent for the determination of bisphenol A, tetrabromobisphenol A, 2,4,6-tribromophenol, and (S)-1,1'-bi-2-naphthol in environmental waters by HPLC, *J. Sep. Sci.* 39 (13) (2016) 2562–2572.
- [57] A. Dabrowski, P. Podkościelny, Z. Hubicki, M. Barczak, Adsorption of phenolic compounds by activated carbon—a critical review, *Chemosphere* 58 (8) (2005) 1049–1070.
- [58] T. Zhang, G. He, F. Dong, Q. Zhang, Y. Huang, Chlorination of enoxacin (ENO) in the drinking water distribution system: Degradation, byproducts, and toxicity, *Sci. Total Environ.* 676 (2019) 31–39.
- [59] Y. Ohko, K.I. Iuchi, C. Niwa, T. Tatsuma, T. Nakashima, T. Iguchi, Y. Kubota, A. Fujishima, 17β-Estradiol degradation by TiO₂ photocatalysis as a means of reducing estrogenic activity, *Environ. Sci. Tech.* 36 (2002) 4175–4181.
- [60] P. Shan, J. Lin, Y. Zhai, S. Dong, Z.T. How, R. Qin, Transformation and toxicity studies of UV filter diethylamino hydroxybenzoyl hexyl benzoate in the swimming pools, *Sci. Total Environ.* 881 (2023) 163498.
- [61] D.O. Mártire, J.A. Rosso, S. Bertolotti, G.C. Le Roux, André M. Braun, M.C. Gonzalez, Kinetic study of the reactions of chlorine atoms and Cl₂• radical anions in aqueous solutions. II. Toluene, Benzoic Acid, and Chlorobenzene, *J. Phys. Chem. A*, 105 (2001) 5385–5392.
- [62] M. Feng, X. Wang, J. Chen, R. Qu, Y. Sui, L. Cizmas, Z. Wang, V.K. Sharma, Degradation of fluoroquinolone antibiotics by ferrate(VI): Effects of water constituents and oxidized products, *Water Res.* 103 (2016) 48–57.
- [63] J. Chen, R. Qu, X. Pan, Z. Wang, Oxidative degradation of triclosan by potassium permanganate: Kinetics, degradation products, reaction mechanism, and toxicity evaluation, *Water Res.* 103 (2016) 215–223.
- [64] X. Wang, J. Hu, Q. Chen, P. Zhang, L. Wu, J. Li, B. Liu, K. Xiao, S. Liang, L. Huang, H. Hou, J. Yang, Synergic degradation of 2,4,6-trichlorophenol in microbial fuel cells with intimately coupled photocatalytic-electrogenic anode, *Water Res.* 156 (2019) 125–135.
- [65] V. Peings, J. Frayret, T. Pigot, Mechanism for the oxidation of phenol by sulfatoferrate(VI): Comparison with various oxidants, *J. Environ. Manage.* 157 (2015) 287–296.
- [66] X. Li, J. Ma, Y. Gao, X. Liu, Y. Wei, Z. Liang, Enhanced atrazine degradation in the Fe(III)/peroxymonosulfate system via accelerating Fe(II) regeneration by benzoquinone, *Chem. Eng. J.* 427 (2022).
- [67] A. Dybala-Defratyka, L. Szatkowski, R. Kaminski, M. Wujec, A. Siwek, P. Paneth, Kinetic isotope effects on dehalogenations at an aromatic carbon, *Environ. Sci. Tech.* 42 (21) (2008) 7744–7750.
- [68] L. Krumina, G. Lyngsie, A. Tunlid, P. Persson, Oxidation of a dimethoxyhydroquinone by ferrihydrite and goethite nanoparticles: iron reduction versus surface catalysis, *Environ. Sci. Tech.* 51 (16) (2017) 9053–9061.
- [69] K. Kasuga, K. Mori, T. Sugimori, M. Handa, Kinetic study on the oxidation of trichlorophenol using hydrogen peroxide and an iron(III) complex of tetrasulfonatophthalocyanine catalyst, *Bull. Chem. Soc. Jpn* 73 (4) (2000) 939–940.
- [70] J. Hu, T. Aizawa, S. Ookubo, Products of aqueous chlorination of bisphenol A and their estrogenic activity, *Environ. Sci. Tech.* 36 (9) (2002) 1980–1987.
- [71] W. Wang, Y. Qian, J. Li, B. Moe, R. Huang, H. Zhang, S.E. Hrudey, X.F. Li, Analytical and toxicity characterization of halo-hydroxyl-benzoquinones as stable halobenzoquinone disinfection byproducts in treated water, *Anal. Chem.* 86 (10) (2014) 4982–4988.
- [72] Z. Zhang, C. Prasse, Chlorination of para-substituted phenols: Formation of α, β-unsaturated C4-dialdehydes and C4-dicarboxylic acids, *J. Environ. Sci.* 117 (2022) 197–208.
- [73] C. Prasse, U. von Gunten, D.L. Sedlak, Chlorination of phenols revisited: unexpected formation of α, β-unsaturated C4-dicarbonyl ring cleavage products, *Environ. Sci. Tech.* 54 (2) (2020) 826–834.
- [74] E.D. Wagner, M.J. Plewa, CHO cell cytotoxicity and genotoxicity analyses of disinfection by-products: An updated review, *J. Environ. Sci.* 58 (2017) 64–76.
- [75] J. Liu, X. Zhang, Comparative toxicity of new halophenolic DBPs in chlorinated saline wastewater effluents against a marine alga: halophenolic DBPs are generally more toxic than haloaliphatic ones, *Water Res.* 65 (2014) 64–72.
- [76] T.W. Schultz, J.W. Yarbrough, Trends in structure–toxicity relationships for carbonyl-containing α, β-unsaturated compounds, SAR and QSAR in Environ. Res. 15 (2004) 139–146.

Supplementary Material

Unveiling the transformation of 2,4,6-trihalophenols by active species in drinking water pipelines: the role of goethite

Feilong Dong^{a,e}, Jiani Zhu^a, Cong Li^b, Eric Lichtfouse^c, Wei Wang^{d*}, Shuang Song^{a*}

^a College of Environment, Zhejiang University of Technology, Hangzhou, 310014, China.

^b School of Environment and Architecture, University of Shanghai for Science and Technology, Shanghai, 200433, China.

^c State Key Laboratory of Multiphase Flow in Power Engineering, Xi'an Jiaotong University, Xi'an, Shaanxi, 710049, China.

^d Department of Environmental Science, College of Environmental and Resource Sciences, Zhejiang University, Hangzhou 310058, China

^e Shaoxing Research Institute, Zhejiang University of Technology, Shaoxing, 312085, China.

*Corresponding author.

Email addresses: ss@zjut.edu.cn

ww1@zju.edu.cn

Text S1 Chemicals and materials

2,4,6-trichlorophenol (TCP) and 2,4,6-tribromophenol (TBP) were purchased from Sigma-Aldrich. 5% of hypochlorous acid solution was purchased from Aladdin Industrial Corporation (Shanghai, China), which was diluted with ultrapure water to obtain the 500 mg/L of hypochlorous acid stock solution. 2, 6-Dichloro-p-quinone was purchased from Tokyo Chemical Industry (Shanghai, China). 90% Dulbecco's modified Eagle medium (DMEM) was prepared using 10% fetal bovine serum (Sabakang) and 1% double antibody. Phosphate buffered saline (PBS) was purchased from Procell (Hubei, China). 3-(4,5)-Dimethylthiaziazolo(-Z-Y1)-3,5-di-phenyltetrazoliumromide (MTT) was purchased from Beijing Solebao Technology Co., LTD. Dimethyl sulfoxide (DMSO) was purchased from Tianjin Fuyu Fine Chemical Co., Ltd. Hexane, acetonitrile and methyl tert-butyl ether (MTBE) of chromatography grade were purchased from Sigma-Aldrich. All other chemicals such as sodium thiosulfate ($\text{Na}_2\text{S}_2\text{O}_3$), tert-butanol (TBA), benzoic acid (BA), and 1,4-dimethoxybenzene (DMOB) were purchased from Sinopharm Chemical Reagent (Shanghai, China). Ultrapure water was obtained from a Milli-Q system with resistivity $> 18 \text{ M}\Omega \cdot \text{cm}$ at $25 \text{ }^\circ\text{C}$.

Text S2 The determination of water quality parameters

DO and pH were measured by a portable multi-parameter meter (HACH HQ 40d). Turbidity was measured using a turbidimeter (HACH 2100Q). The concentrations of TCP and TBP were determined using high performance liquid chromatography (HPLC; Waters Corporation, USA) equipped with Waters 2489 UV/Vis detector and XDB-C18 chromatographic column (150 mm \times 4.6 mm, 5 μm , Agilent Zorbax).

Text S3 Analytical methods

The concentrations of TCP and TBP were determined using high performance liquid chromatography (HPLC; Waters Corporation, USA) equipped with Waters 2489 UV/Vis detector and XDB-C18 chromatographic column (150 mm × 4.6 mm, 5 μm, Agilent Zorbax). The mobile phases for TCP analysis were acetonitrile and an ultrapure aqueous solution (pH=3.0) with phosphoric acid at a ratio of 80:20 (v/v), the detector wavelength was set at 295 nm, the column temperature was maintained at 30 °C, and the flow rate was 0.6 mL/min. The mobile phases for TBP analysis were acetonitrile and ultrapure aqueous solution containing 0.1% perchloric acid at a ratio of 65:35 (v/v), the detector wavelength was at 230 nm, the column temperature was maintained at 30 °C, and the flow rate was 0.8 mL/min.

The intermediate products of TCP and TBP were identified by high performance liquid chromatography-mass spectrometry (HPLC-MS, Agilent qtof6550). The mobile phase was acetonitrile: water (90:10, v/v) spiked with 0.1% formic acid at a flow rate of 0.3 mL/min. The MS system was operated in ESI+ mode with a capillary voltage of 4 kV and a gas temperature of 150 °C. The drying gas was 15 L/min, the temperature of the jacket gas was 350 °C, and the flow rate of the jacket gas was 12 L/min. The m/z range was from 100 to 500, and the scan time was 0.1 s.

The concentrations of the aliphatic DBPs were analyzed using gas chromatography equipped with an electron capture detector (GC-ECD) (GC-450, Varian, Palo Alto, CA, USA) and a DB-5 capillary column (30 m×0.25 mm×0.25 μm) [1,2]. The initial temperature of the oven was held at 35 °C for 10 min, then warming up to 80 °C at 10 °C/min, thereby warming up to 150 °C at 20 °C/min [2,3]. The temperatures of the splitless injector and detector were 210 and 290°C, respectively.

In addition, the chlorine concentration was determined by N,N-diethyl-p-phenylenediamine (DPD) colorimetric method with a free chlorine kit (HACH DR300). An electron paramagnetic resonance (EPR) spectrometer (Bruker EMX PLUS, Germany) was employed to determine the species of free radicals generated by chlorination. DMPO was used as a trapping agent for •OH, ClO• and Cl•. The goethite was characterized using XRD (XPert Pro MPD; PANalytical B.V., Netherlands) analysis with Cu Kα radiation (λ = 0.154 nm) and X-ray photoelectron spectroscopy (XPS, PHI 5000C ESCA, Perkin-Elmer, USA) with an Al Kα X-ray source (hν = 1486.6 eV).

Text S4 The methods of DFT calculation

All quantum chemical calculations were performed on a Gaussian 03 package based on density functional theory (DFT) [4]. The structure of 2,4,6-trihalophenols (e.g., 2,4,6-Trichlorophenol and 2,4,6-Tribromophenol) were optimized using the hybrid B3LYP/6-311++G (d,p) method. Besides, this study calculated the $2FED^2_{HOMO}$ of each atom on 2,4,6-trihalophenols molecule. The high values of highest occupied molecular orbital (HOMO) are considered to be the most prone to electrophilic reactions [5]. The calculation considered the effect of reaction solvent (i.e., water) by using “pop = reg”.

Text S5 The methods of cytotoxicity analysis

The Chinese hamster ovary (CHO) cells was employed to evaluate the cytotoxicity variation in the degradation process of TCP and TBP, since the cell line has been widely used in comparison of the toxicity of DBPs and abundant relevant data were available. The water sampled during the experiments of TCP and TBP was used to detect the relative viabilities. Before toxicity analysis, the samples and consumables were autoclaved in an autoclave to avoid the interference of microorganisms. The CHO cells were taken and counted in the logarithmic growth phase. The cells were seeded into 96-well plates at 8×10^3 /well, and cultured in a 5% CO₂ incubator at 37 °C until the cells adhered. After culturing for 72 h, the medium containing the sample was removed. Each well was washed three times using PBS, and 100 μL of medium containing 0.5 mg/mL MTT was added to each well. Then 96-well plates were incubated in 5% CO₂ and 37°C incubators for 4.0 h. Finally, 100 μL of DMSO was added to each well after discarding the supernatant. After 10 min of gentle shaking, the absorbance at 570 nm was detected using a microplate reader (TECAN, model: SPARK 10 M), and the cell viability was determined.

Text S6 The identification of iron species.

To identify Fe species produced by goethite dissolution, we firstly determined the concentrations of Fe²⁺ and Fe³⁺ in water and goethite. The removal of TCP/TBP was conducted in darkness with headspace-free glass bottles, the initial concentrations of TCP and TBP were 2 μmol/L, free chlorine (HClO/ClO⁻) and goethite were 2.0 mg/L and 4.0 g/L, respectively. Results shown that Fe²⁺ and Fe³⁺ were not observed above the detection limitation of 50.0 μg/L. As a consequence, 50.0 μg/L of Fe²⁺ and 50.0 μg/L of Fe³⁺ were used to activate HClO/ClO⁻ in additional experiments. As show in Fig. S2, negligible removal of TCP/TBP was found after 8 min of reaction. The results demonstrated that the goethite dissolution had neglected effect to the TCP/TBP elimination in our experiments.

Text S7 The intermediates of TCP during the direct oxidation with goethite.

To elucidate the surface chemical process of goethite, direct oxidation of TCP with goethite was conducted in a separate experiment. The removal of TCP in the presence of goethite was performed at pH 7.5 ± 0.1 and 25 °C. TCP was conducted in batch-scale pipe reactor, the initial goethite concentration was 4.0 g/L and initial TCP concentration was 2.0 μmol/L. At the reaction of 24 h, the removal of TCP and intermediates were detected in the reaction solution. Subsequently, the goethite used in the experiment was washed with methanol, and the leached components were detected, as illustrated in Fig. S4.

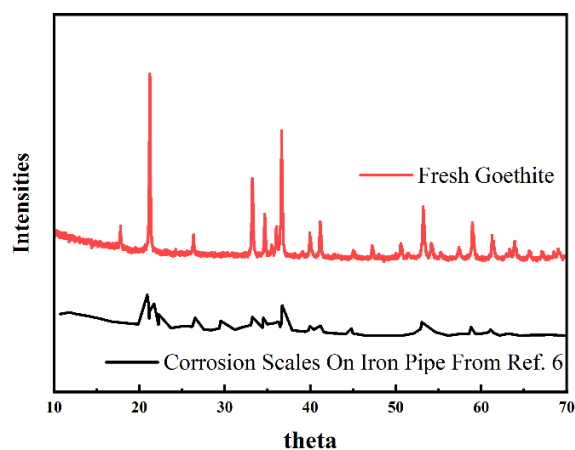


Fig. S1. The XRD patterns of the goethite and corrosion scales on iron pipe. The peak of corrosion scale was referred from Wang et al [6].

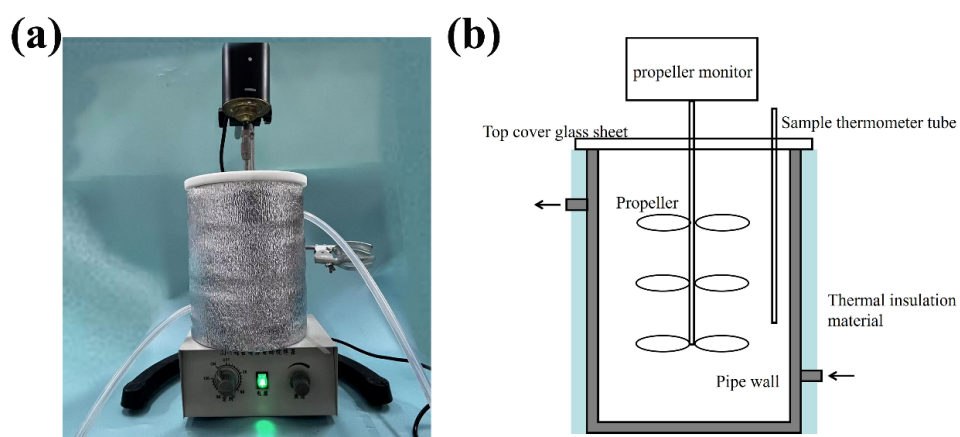


Fig. S2. Schematic diagram of batch-scale pipe reactor used for goethite mediated chlorination. (Experimental conditions: Reaction time = 8.0 min, temperature = $25 \pm 1^\circ\text{C}$, initial pH = 7.5 ± 0.1 , initial goethite concentration = 4.0 g/L, initial free chlorine concentration = 2.0 mg/L, initial TCP and TBP concentration = 2.0 $\mu\text{mol/L}$).

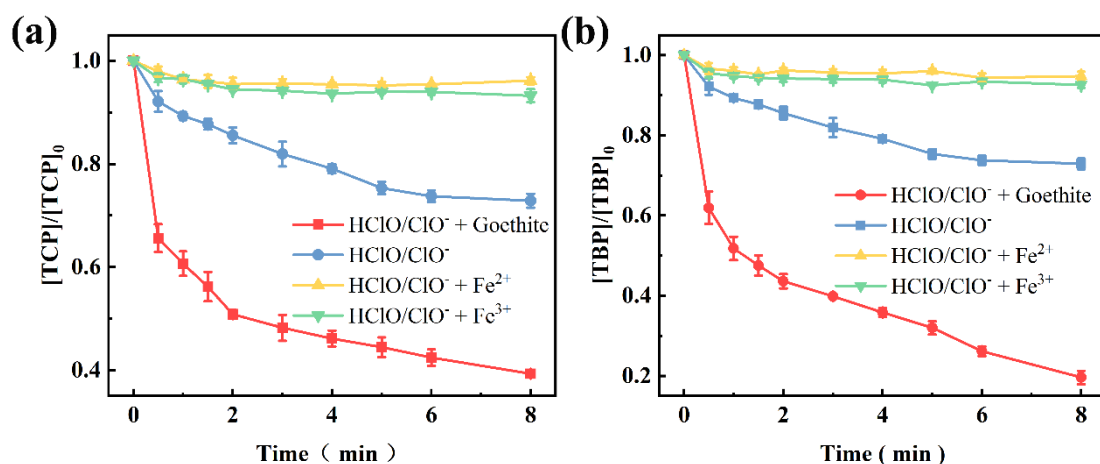


Fig. S3. The degradation of (a) TCP and (b) TBP during chlorination with the existence of goethite, free chlorine, and iron ion in batch-scale pipe reactor. (Experimental conditions: Reaction time = 8.0 min, temperature = $25 \pm 1^\circ\text{C}$, initial pH = 7.5 ± 0.1 , initial goethite concentration = 4.0 g/L, initial free chlorine concentration = 2.0 mg/L, initial TCP and TBP concentration = 2.0 $\mu\text{mol/L}$, initial iron ion concentration = 50.0 $\mu\text{g/L}$).

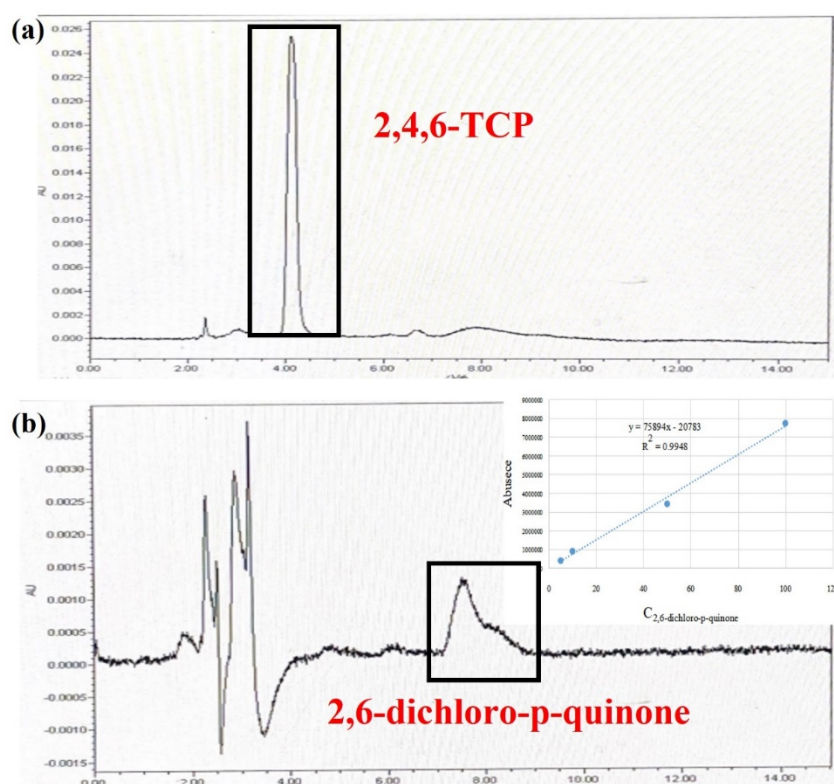


Fig. S4. The HPLC spectra of (a) TCP and (b) 2,6-dichloro-p-quinone with the existence of goethite in batch-scale pipe reactor. (Experimental conditions: Reaction time = 24.0 h, temperature = $25 \pm 1^\circ\text{C}$, initial pH = 7.5 ± 0.1 , initial goethite concentration = 4.0 g/L, initial TCP concentration = 2.0 $\mu\text{mol/L}$).

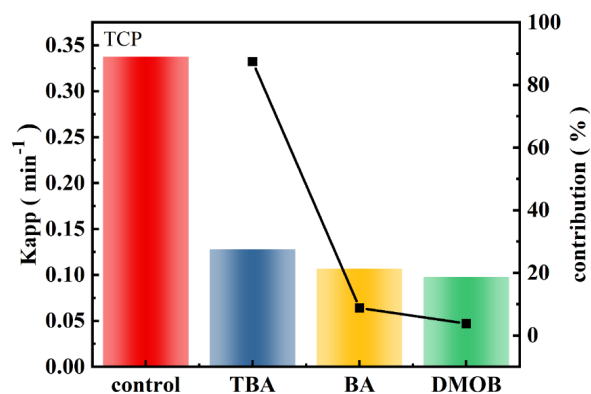


Fig. S5. The rate constants for degradation of TCP (columns, primary y-axis); contribution of active species for TCP (symbols, secondary y-axis) removal during the goethite-mediated chlorination in batch-scale pipe reactor. (Experimental conditions: Reaction time = 8.0 min, temperature = $25 \pm 1^\circ\text{C}$, initial pH = 7.5 ± 0.1 , initial goethite concentration = 4.0 g/L, initial free chlorine concentration = 2.0 mg/L, initial TCP concentration = 2.0 $\mu\text{mol/L}$)

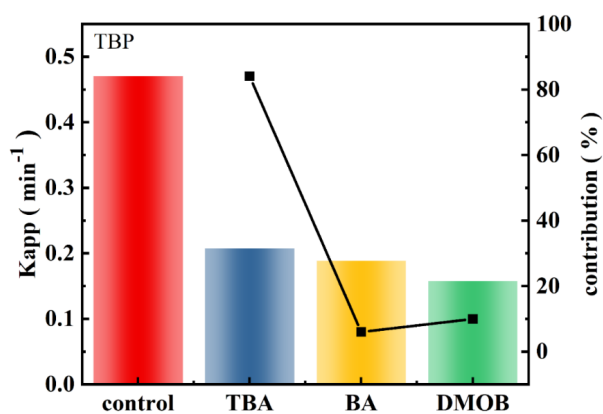


Fig. S6. The rate constants for degradation of TBP (columns, primary y-axis); contribution of active species for TBP (symbols, secondary y-axis) removal during the goethite mediated chlorination in batch-scale pipe reactor. (Experimental conditions: Reaction time = 8.0 min, temperature = $25 \pm 1^\circ\text{C}$, initial pH = 7.5 ± 0.1 , initial goethite concentration = 4.0 g/L, initial free chlorine concentration = 2.0 mg/L, initial TBP concentration = 2.0 $\mu\text{mol/L}$)

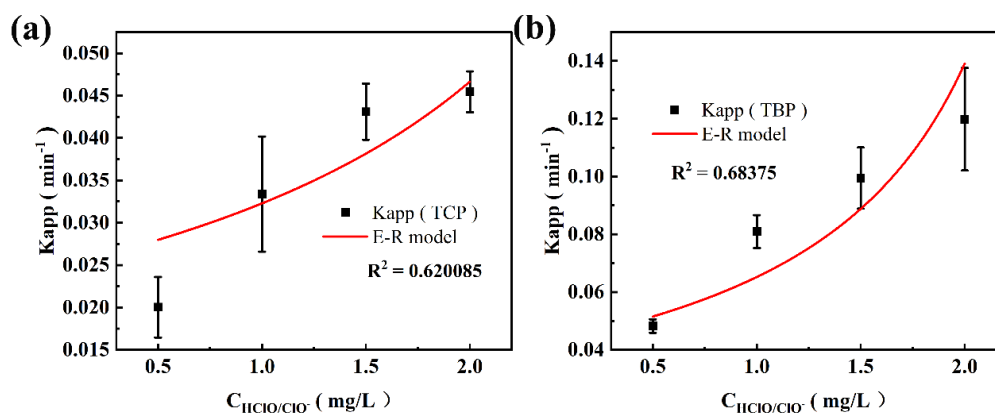


Fig. S7. E-R model fit diagram for initial chlorine concentration changes of (a) TCP and (b) TBP during the goethite mediated chlorination in batch-scale pipe reactor. (Experimental conditions: Reaction time = 8.0 min, temperature = $25 \pm 1^\circ\text{C}$, initial pH = 7.5 ± 0.1 , initial goethite concentration = 4.0 g/L, initial free chlorine concentration = 2.0 mg/L, initial TCP and TBP concentration = 2.0 $\mu\text{mol/L}$).

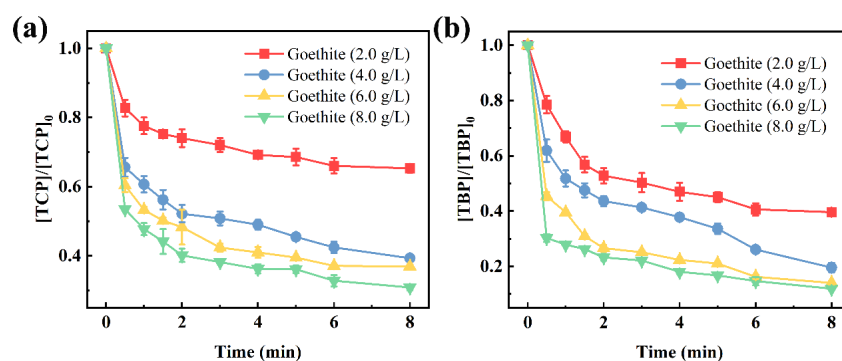


Fig. S8. Effect of goethite on the degradation of (a) TCP and (b) TBP during the goethite mediated chlorination in batch-scale pipe reactor. (Experimental conditions: Reaction time = 8.0 min, temperature = $25 \pm 1^\circ\text{C}$, initial pH = 7.5 ± 0.1 , initial free chlorine concentration = 2.0 mg/L, initial TCP and TBP concentration = 2.0 $\mu\text{mol/L}$).

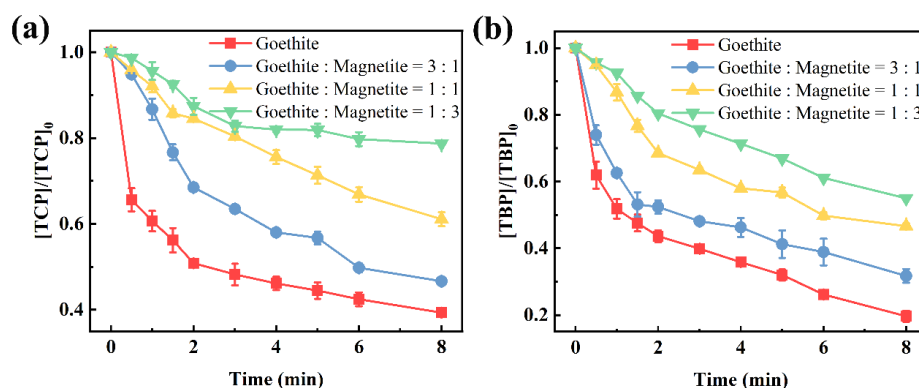


Fig. S9. Effect of the ratio of goethite to magnetite on the degradation of (a) TCP and (b) TBP during the goethite mediated chlorination in batch-scale pipe reactor. (Experimental conditions: Reaction time = 8.0 min, temperature = $25 \pm 1^\circ\text{C}$, initial pH = 7.5 ± 0.1 , initial free chlorine concentration = 2.0 mg/L, initial TCP and TBP concentration = 2.0 $\mu\text{mol/L}$).

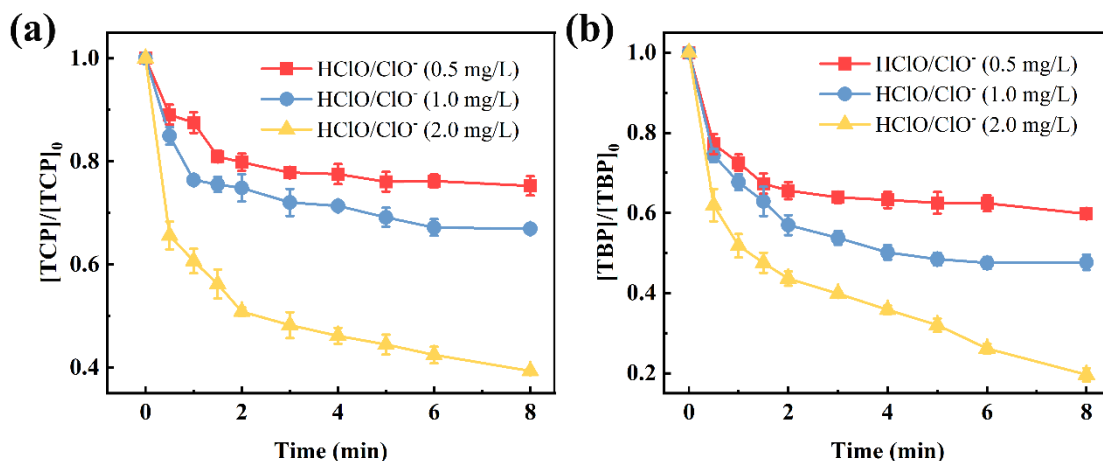


Fig. S10. Effect of free chlorine on the degradation of (a) TCP and (b) TBP during the goethite mediated chlorination in batch-scale pipe reactor. (Experimental conditions: Reaction time = 8.0 min, temperature = $25 \pm 1^\circ\text{C}$, initial pH = 7.5 ± 0.1 , initial goethite concentration = 4.0 g/L, initial TCP and TBP concentration = 2.0 $\mu\text{mol/L}$).

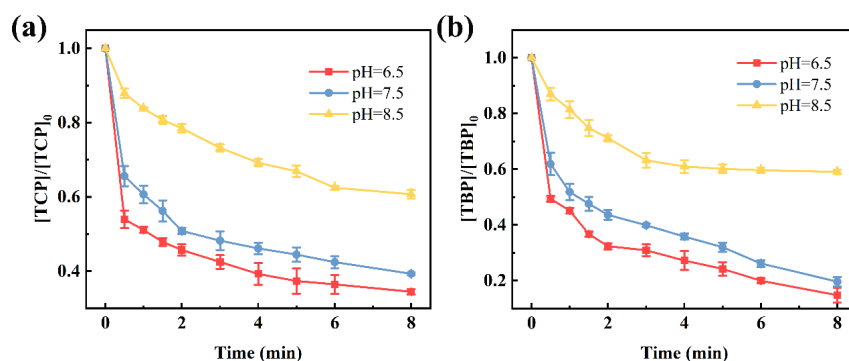


Fig. S11. Effect of pH on the degradation of (a) TCP and (b) TBP during the goethite mediated chlorination in batch-scale pipe reactor. (Experimental conditions: Reaction time = 8.0 min, temperature = $25 \pm 1^\circ\text{C}$, initial goethite concentration = 4.0 g/L, initial free chlorine concentration = 2.0 mg/L, initial TCP and TBP concentration = 2.0 $\mu\text{mol/L}$).

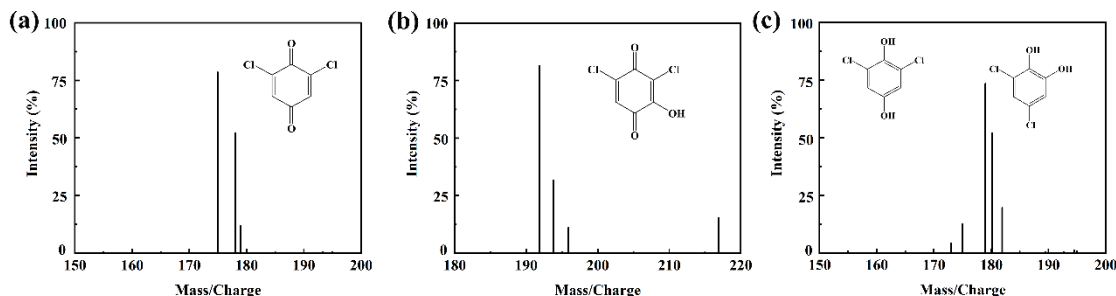


Fig. S12. The intermediates were generated by TCP degradation during chlorination alone in batch-scale pipe reactor with the help of LC-MS. (Experimental conditions: Reaction time = 1.0 h, temperature = $25 \pm 1^\circ\text{C}$, initial pH = 7.5 ± 0.1 , initial free chlorine concentration = 2.0 mg/L, initial TCP concentration = 2.0 $\mu\text{mol/L}$).

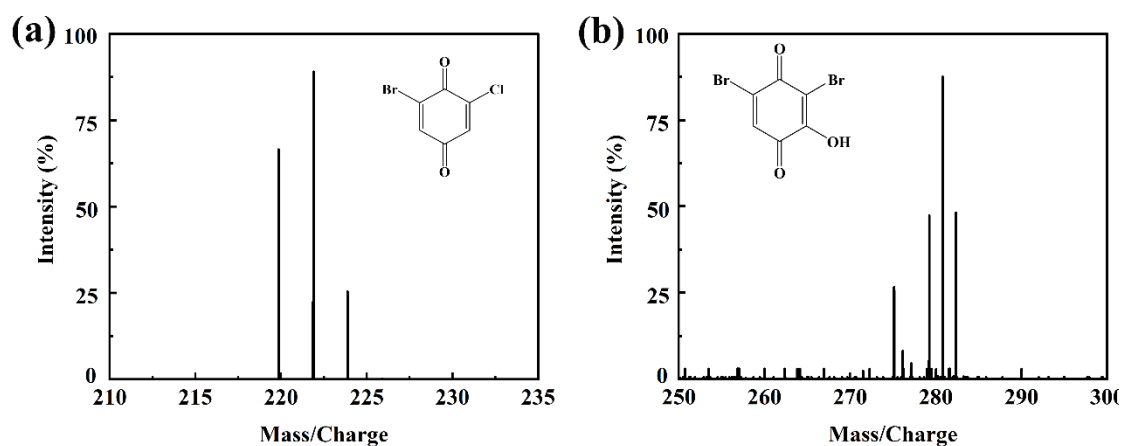


Fig. S13. The intermediates were generated by TBP degradation during chlorination alone in batch-scale pipe reactor with the help of LC-MS. (Experimental conditions: Reaction time = 1.0 h, temperature = $25 \pm 1^\circ\text{C}$, initial pH = 7.5 ± 0.1 , initial free chlorine concentration = 2.0 mg/L, initial TBP concentration = 2.0 $\mu\text{mol/L}$).

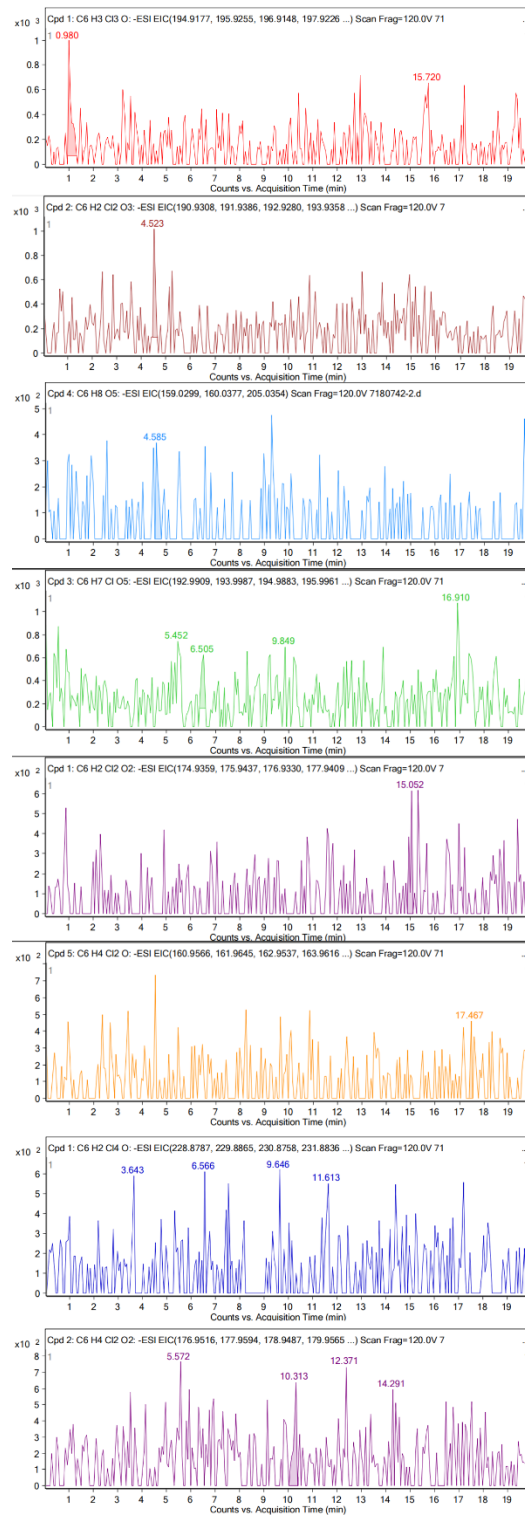


Fig. S14. The LC-MS chromatogram spectra of TCP intermediates during the goethite mediated chlorination in batch-scale pipe reactor with the help of LC-MS. (Experimental conditions: Reaction time = 1.0 h, temperature = $25 \pm 1^\circ\text{C}$, initial pH = 7.5 ± 0.1 , initial goethite concentration = 4.0 g/L, initial free chlorine concentration = 2.0 mg/L, initial TCP concentration = 2.0 $\mu\text{mol/L}$).

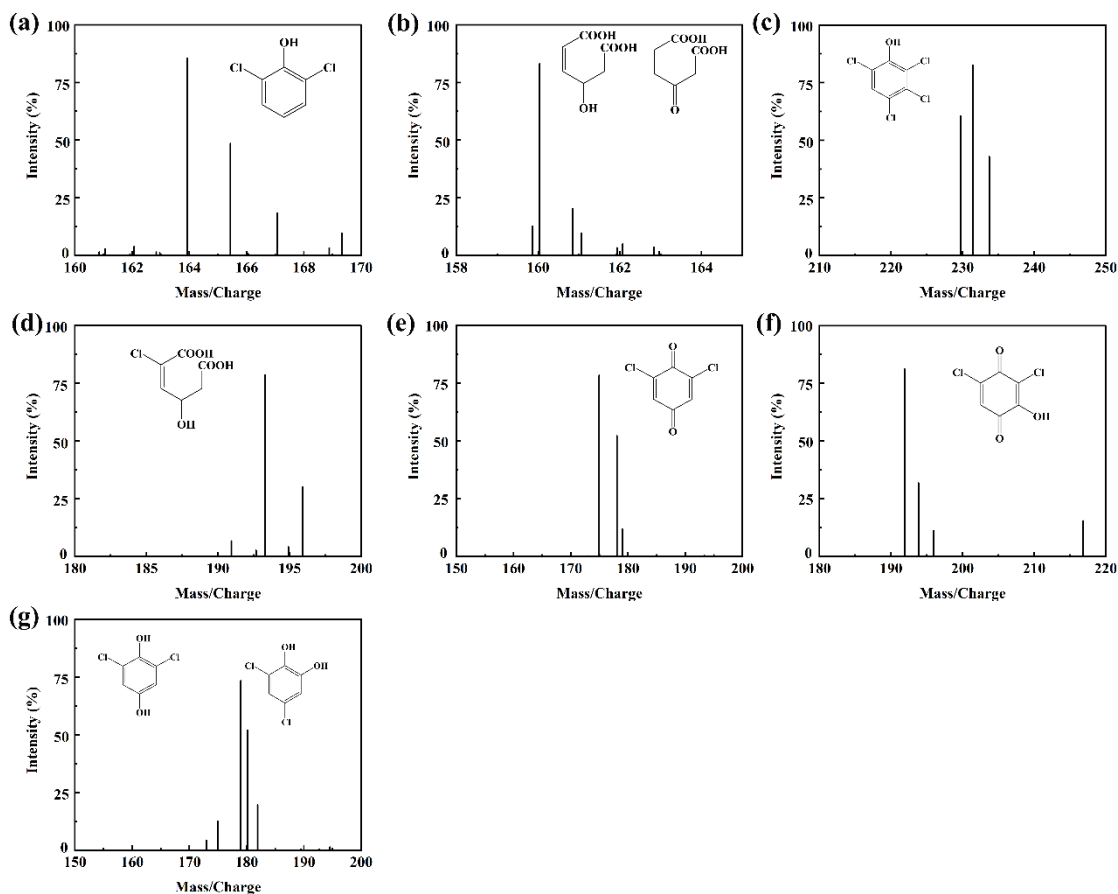


Fig. S15. The intermediates were generated by TCP degradation during the goethite mediated chlorination in batch-scale pipe reactor with the help of LC-MS. (Experimental conditions: Reaction time = 1.0 h, temperature = $25 \pm 1^\circ\text{C}$, initial pH = 7.5 ± 0.1 , initial goethite concentration = 4.0 g/L, initial free chlorine concentration = 2.0 mg/L, initial TCP concentration = 2.0 $\mu\text{mol/L}$).

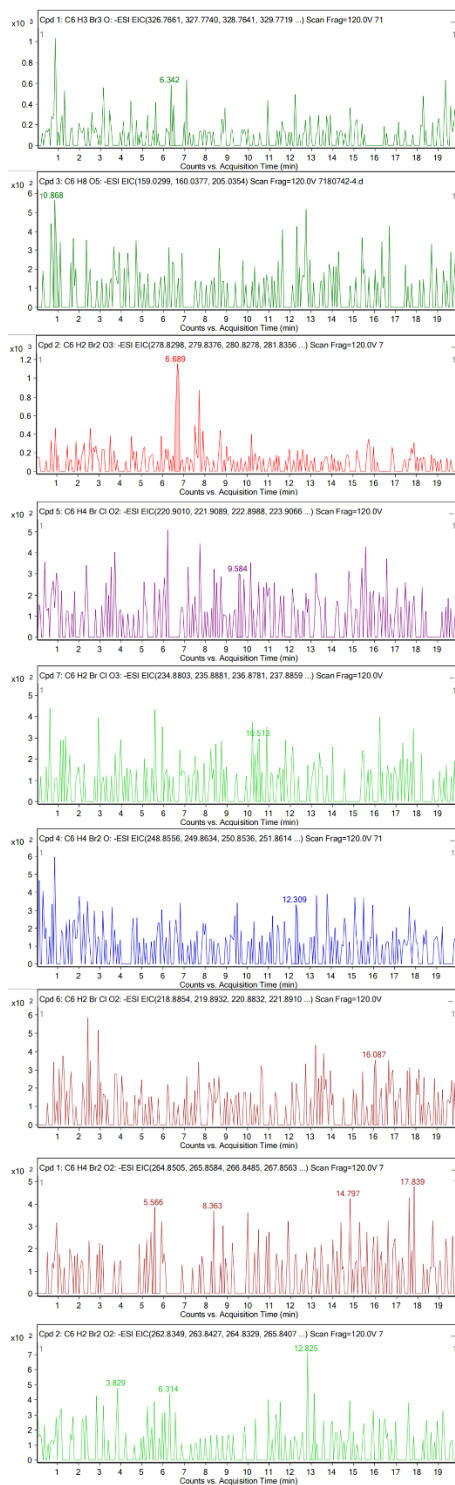


Fig. S16. The LC-MS chromatogram spectra of TBP intermediates during the goethite mediated chlorination in batch-scale pipe reactor with the help of LC-MS. (Experimental conditions: Reaction time = 1.0 h, temperature = $25 \pm 1^\circ\text{C}$, initial pH = 7.5 ± 0.1 , initial goethite concentration = 4.0 g/L, initial free chlorine concentration = 2.0 mg/L, initial TBP concentration = 2.0 $\mu\text{mol/L}$).

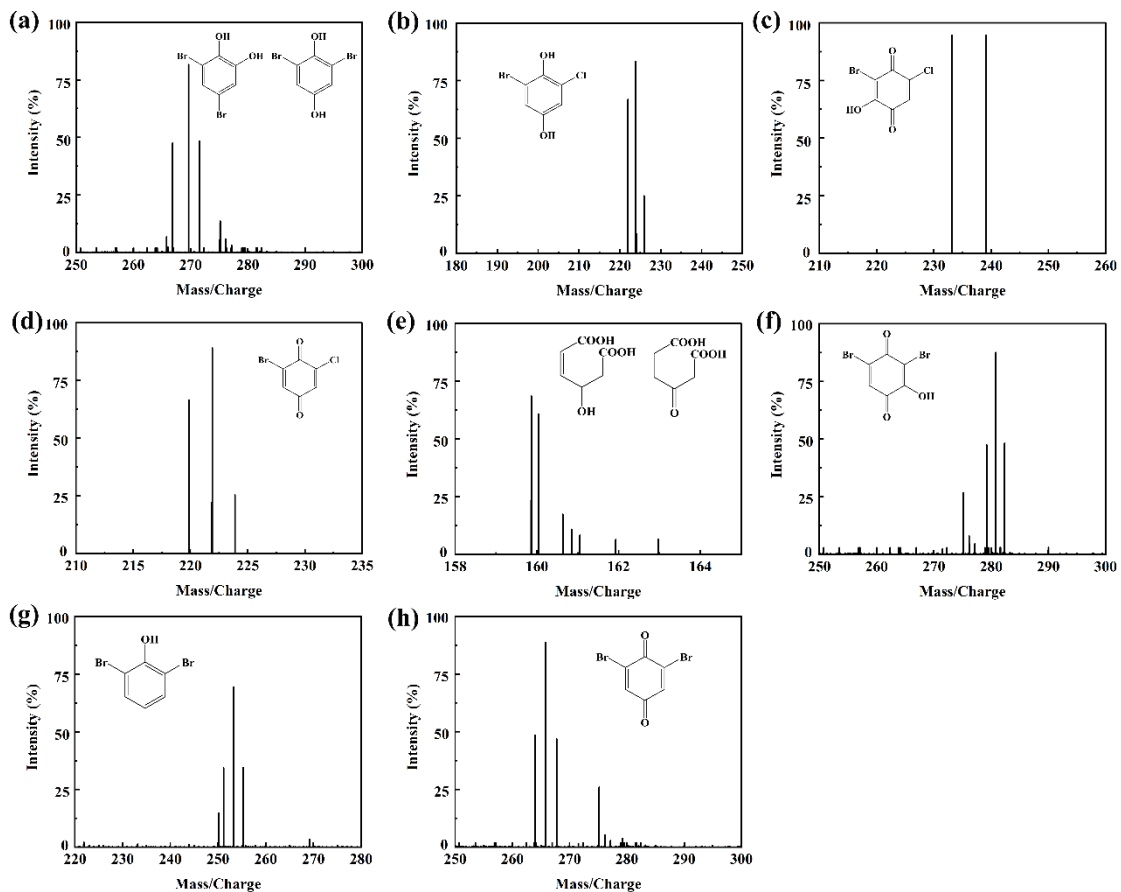


Fig. S17. The intermediates were generated by TBP degradation during the goethite mediated chlorination in batch-scale pipe reactor with the help of LC-MS. (Experimental conditions: Reaction time = 1.0 h, temperature = $25 \pm 1^\circ\text{C}$, initial pH = 7.5 ± 0.1 , initial goethite concentration = 4.0 g/L, initial free chlorine concentration = 2.0 mg/L, initial TBP concentration = 2.0 $\mu\text{mol/L}$).

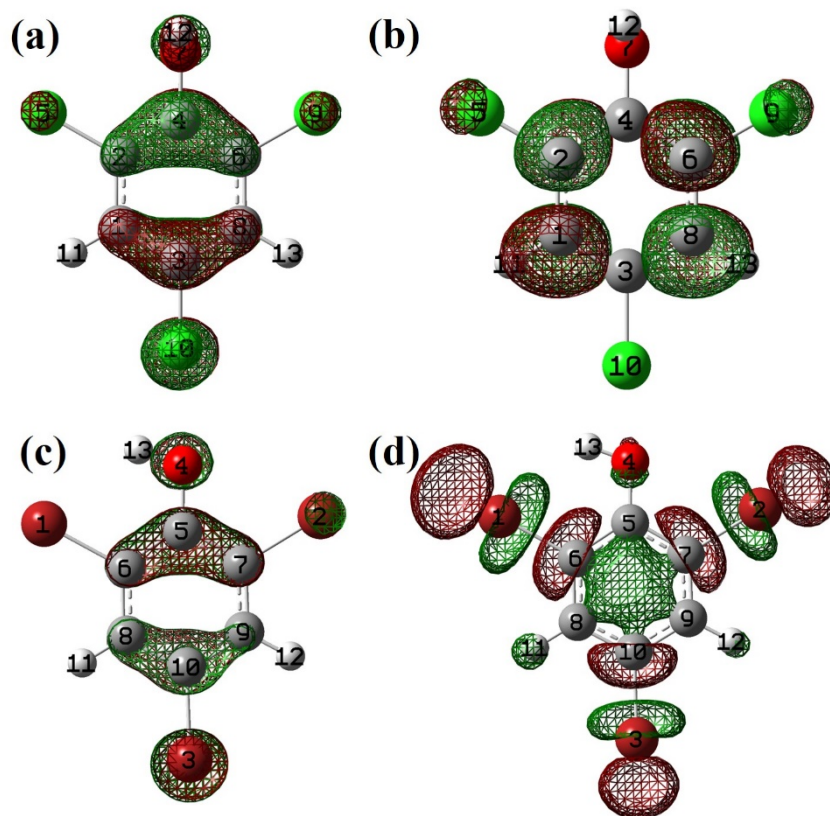


Fig. S18. The LUMO (a) and HOMO (b) orbitals of TCP; The LUMO (c) and HOMO (d) orbitals of TBP.

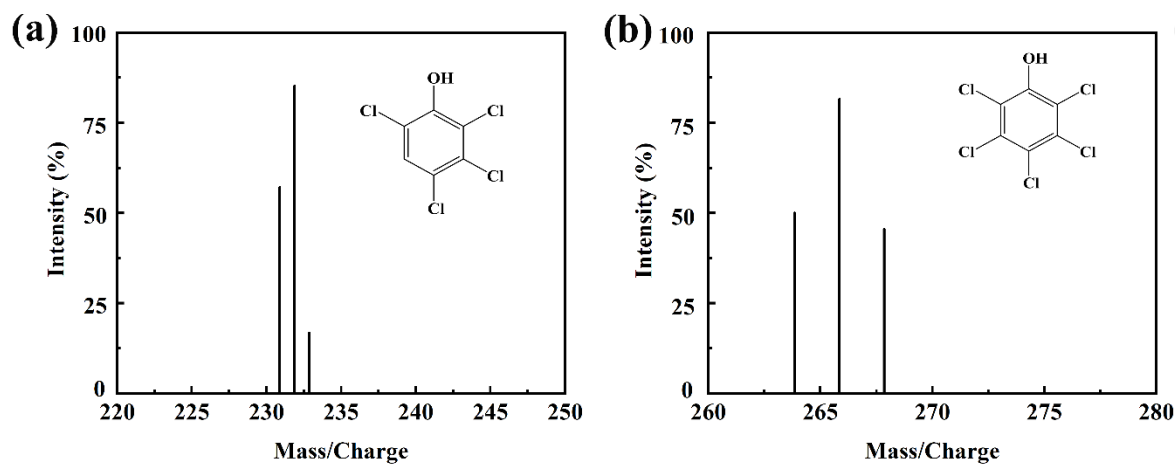


Fig. S19. The intermediates were generated by TCP degradation after addition of TBA during the goethite mediated chlorination in batch-scale pipe reactor with the help of LC-MS. (Experimental conditions: Reaction time = 1.0 h, temperature = $25 \pm 1^\circ\text{C}$, initial pH = 7.5 ± 0.1 , initial goethite concentration = 4.0 g/L, initial free chlorine concentration = 2.0 mg/L, initial TCP concentration = 2.0 $\mu\text{mol/L}$, initial TBA concentration = 150.0 $\mu\text{mol/L}$).

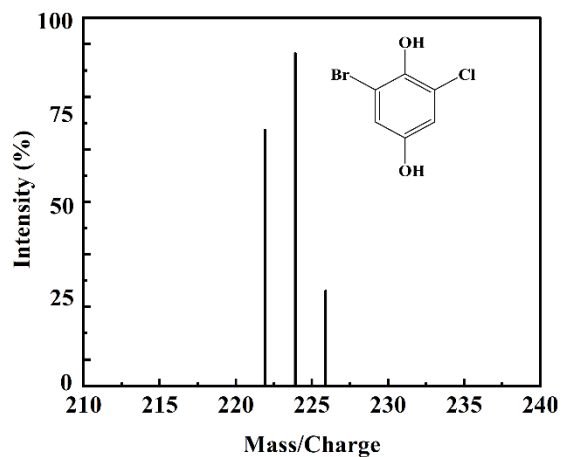


Fig. S20. The intermediates were generated by TBP degradation after addition of TBA during the goethite mediated chlorination in batch-scale pipe reactor with the help of LC-MS. (Experimental conditions: Reaction time = 1.0 h, temperature = $25 \pm 1^\circ\text{C}$, initial pH = 7.5 ± 0.1 , initial goethite concentration = 4.0 g/L, initial free chlorine concentration = 2.0 mg/L, initial TBP concentration = 2.0 $\mu\text{mol/L}$, initial TBA concentration = 150.0 $\mu\text{mol/L}$).

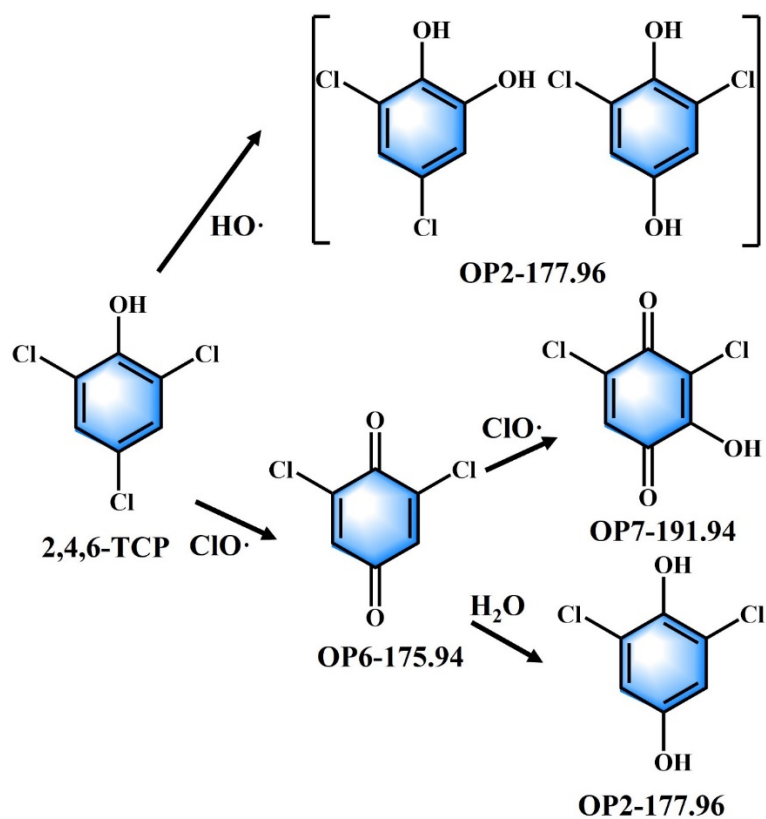


Fig. S21. The proposed pathways of TCP chlorination alone in batch-scale pipe reactor. (Experimental conditions: Reaction time = 1.0 h, temperature = $25 \pm 1^\circ\text{C}$, initial pH = 7.5 ± 0.1 , initial free chlorine concentration = 2.0 mg/L, initial TCP concentration = 2.0 $\mu\text{mol/L}$).

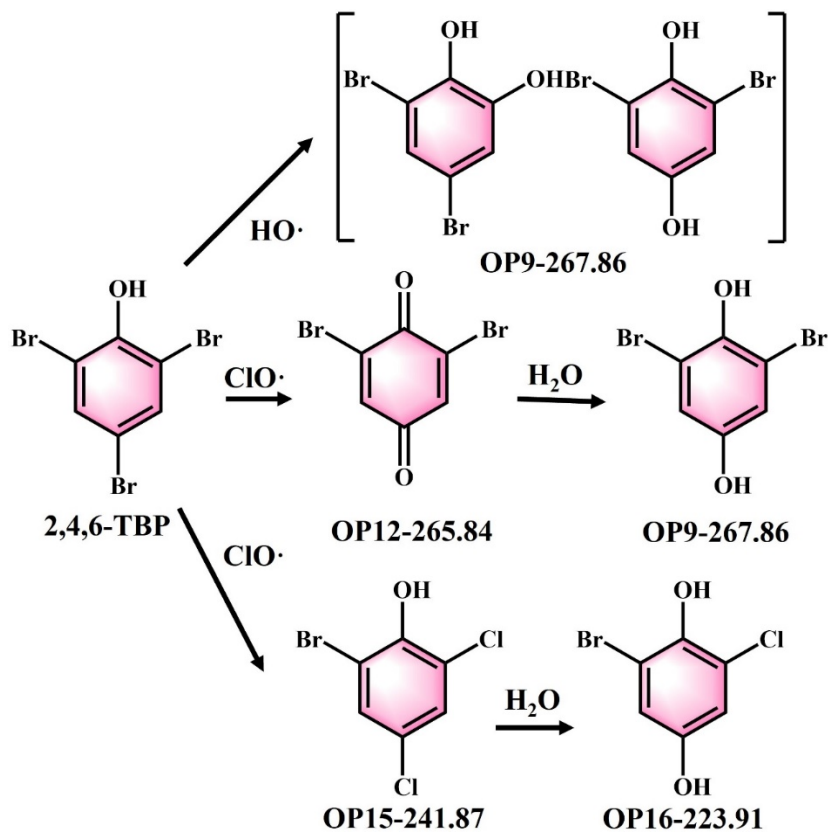


Fig. S22. The proposed pathways of TBP chlorination alone in batch-scale pipe reactor. (Experimental conditions: Reaction time = 1.0 h, temperature = $25 \pm 1^\circ\text{C}$, initial pH = 7.5 ± 0.1 , initial free chlorine concentration = 2.0 mg/L, initial TBP concentration = 2.0 $\mu\text{mol/L}$).

Table S1. The water quality parameters of the tap water.

Water quality parameters	Content
residual chlorine (as Cl ₂)	0.3 ± 0.1 mg/L
pH value	7.5 ± 0.1
DO	9.2 ± 0.4 mg/L
TCP	Not detected
TBP	Not detected

Table S2. The K_{app} of TCP and TBP during the goethite mediated chlorination in batch-scale pipe reactor. (Experimental conditions: Reaction time = 8.0 min, temperature = $25 \pm 1^\circ\text{C}$, initial pH = 7.5 ± 0.1).

	TCP	TBP
$C_{\text{HClO}/\text{ClO}^-}$ (mg/L)	K_{APP} (Min ⁻¹)	K_{APP} (Min ⁻¹)
0.0	0.14127 ± 0.04979	0.18149 ± 0.01336
0.5	0.12225 ± 0.00157	0.25752 ± 0.00465
1.0	0.23420 ± 0.00050	0.37766 ± 0.00425
2.0	0.33996 ± 0.00145	0.47673 ± 0.00361
3.0	0.41672 ± 0.00025	0.53444 ± 0.00238
$C_{\text{TCP/TBP}}$ ($\mu\text{mol/L}$)	K_{APP} (Min ⁻¹)	K_{APP} (Min ⁻¹)
0.5	0.06975 ± 0.00385	0.17650 ± 0.00484
1.0	0.18306 ± 0.00117	0.32359 ± 0.00168
2.0	0.33996 ± 0.00145	0.47673 ± 0.00361
3.0	0.41672 ± 0.00600	0.56110 ± 0.00345
C_{goethite} (g/L)	K_{APP} (Min ⁻¹)	K_{APP} (Min ⁻¹)
0.0	0.08448 ± 0.02104	0.14712 ± 0.00603
2.0	0.18370 ± 0.00242	0.37155 ± 0.00710
4.0	0.33996 ± 0.00145	0.47673 ± 0.00361
6.0	0.43910 ± 0.00181	0.73165 ± 0.00163
8.0	0.51522 ± 0.00094	0.81905 ± 0.00158

Table S3. The intermediate product of TBP produced in during the goethite mediated chlorination in darkness with headspace-free glass bottles with the help of LC-MS. (Experimental conditions: Reaction time = 1.0 h, temperature = $25 \pm 1^\circ\text{C}$, initial pH = 7.5 ± 0.1 , initial goethite concentration = 4.0 g/L, initial free chlorine concentration = 2.0 mg/L, initial TBP concentration = 2.0 $\mu\text{mol/L}$).

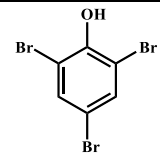
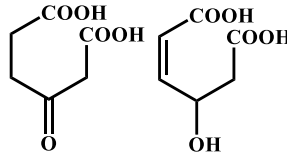
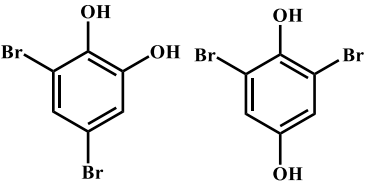
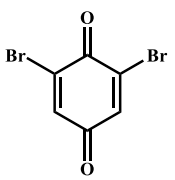
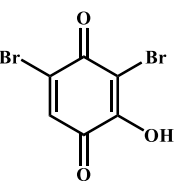
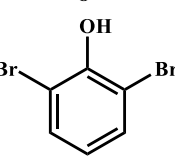
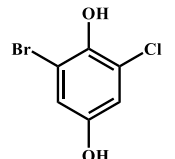
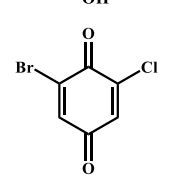
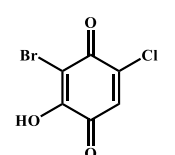
Compounds	M/Z	Chemical formula	Structural formula
TBP	328.80	$\text{C}_6\text{H}_3\text{Br}_3\text{O}$	
OP5-160.04	160.04/205.04	$\text{C}_6\text{H}_8\text{O}_5$	
OP9-267.86	266.84	$\text{C}_6\text{H}_4\text{O}_2\text{Br}_2$	
OP12-265.84	265.83	$\text{C}_6\text{H}_2\text{O}_2\text{Br}_2$	
OP13-281.84	280.83	$\text{C}_6\text{H}_2\text{O}_3\text{Br}_2$	
OP14-281.86	250.85	$\text{C}_6\text{H}_4\text{OBr}_2$	
OP16-223.91	223.91	$\text{C}_6\text{H}_4\text{ClBrO}_2$	
OP17-221.89	221.89/266.90	$\text{C}_6\text{H}_2\text{ClBrO}_2$	
OP18-235.89	237.86/282.89	$\text{C}_6\text{H}_2\text{ClBrO}_3$	

Table S4. The intermediate product of TCP produced during the goethite mediated chlorination in batch-scale pipe reactor with the help of LC-MS. (Experimental conditions: Reaction time = 1.0 h, temperature = $25 \pm 1^\circ\text{C}$, initial pH = 7.5 ± 0.1 , initial goethite concentration = 4.0 g/L, initial free chlorine concentration = 2.0 mg/L, initial TCP concentration = 2.0 $\mu\text{mol/L}$).

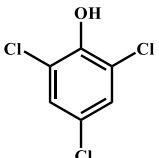
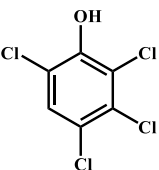
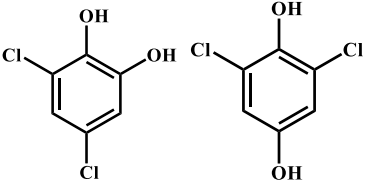
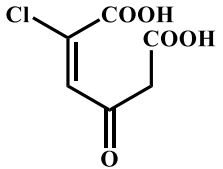
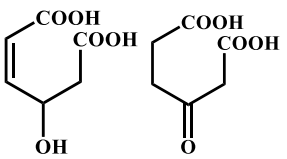
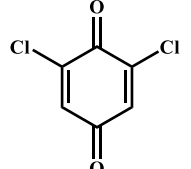
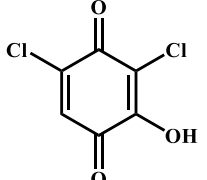
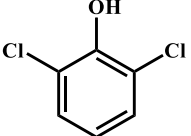
Compounds	M/Z	Chemical formula	Structural formula
TCP	197.40	$\text{C}_6\text{H}_3\text{Cl}_3\text{O}$	
OP1-231.88	230.87/276.88	$\text{C}_6\text{H}_2\text{OCl}_4$	
OP2-177.96	176.95/222.96	$\text{C}_6\text{H}_4\text{O}_2\text{Cl}_2$	
OP4-194.00	192.99	$\text{C}_6\text{H}_7\text{O}_5\text{Cl}$	
OP5-160.04	159.03	$\text{C}_6\text{H}_8\text{O}_5$	
OP6-175.94	174.94	$\text{C}_6\text{H}_2\text{O}_2\text{Cl}_2$	
OP7-191.94	190.93	$\text{C}_6\text{H}_2\text{O}_3\text{Cl}_2$	
OP8-161.96	160.95/206.96	$\text{C}_6\text{H}_4\text{OCl}_2$	

Table S5. Second-order rate constants ($M^{-1}s^{-1}$) of radicals toward probe compounds.

	$k_{HO\cdot}$	$k_{Cl\cdot}$	$k_{ClO\cdot}$	References
NB	3.9×10^9			[7,8]
BA	5.9×10^9	1.8×10^{10}	$< 10^7$	[8-11]
DMOB	7.0×10^9	1.8×10^{10}	2.1×10^9	[11,12]

Table S6. The K_{app} of TCP and TBP during the goethite mediated chlorination in batch-scale pipe reactor. (Experimental conditions: Reaction time = 8.0 min, temperature = $25 \pm 1^\circ\text{C}$, initial pH = 7.5 ± 0.1 , initial TCP and TBP concentration = $2.0 \mu\text{mol/L}$).

Condition	TCP	TBP
	K_{APP} (Min^{-1})	K_{APP} (Min^{-1})
No scavenger	0.33996 ± 0.00145	0.47673 ± 0.00361
TBA ($150 \mu\text{M}$)	0.12782 ± 0.05793	0.20713 ± 0.05793
BA ($150 \mu\text{M}$)	0.10680 ± 0.04896	0.18842 ± 0.04896
DMOB ($150 \mu\text{M}$)	0.09770 ± 0.05771	0.15732 ± 0.05771

Table S7. The relative contribution rates of active species. (The sum of all relative contribution rates is 100%)

Contribution (%)	TCP	TBP
•OH	87.4421	84.0740
Cl•	8.76381	5.98222
ClO•	3.79404	9.94373

Table S8. Calculation of K of TCP and TBP in reaction system by L-H model during the goethite mediated chlorination i in batch-scale pipe reactor. (Experimental conditions: Reaction time = 8.0 min, temperature = $25 \pm 1^\circ\text{C}$, initial pH = 7.5 ± 0.1 , initial goethite concentration = 4.0 g/L, initial free chlorine concentration = 2.0 mg/L, initial TCP and TBP concentration = 2.0 $\mu\text{mol/L}$).

	TCP	TBP
K ($\text{mol} \cdot \text{L}^{-1} \cdot \text{S}^{-1}$)	4.2046×10^{-5}	3.0885×10^{-4}
$K_{TCP/TBP}$ ($\text{L} \cdot \text{mol}^{-1}$)	4.7130×10^5	1.9848×10^5
$K_{\text{HClO}/\text{ClO}^-}$ ($\text{L} \cdot \text{mol}^{-1}$)	7.3856×10^4	9.3572×10^4

Table S9. The DFT calculation of Frontier electron densities on the atoms in TCP and TBP, calculated using the UB3LYP/6-311++G (d, p) method.

TCP					TBP				
No.	Atom	Charge	2FED ² _{HOMO}	2FED ² _{LUMO}	No.	Atom	Charge	2FED ² _{HOMO}	2FED ² _{LUMO}
1	C	-1.379	6.065	1177	1	Br	-0.109	0.002	3.611
2	C	1.444	2.229	1924	2	Br	-0.055	0.239	2.605
3	C	0.761	0.287	1563	3	Br	-0.116	0.027	15.82
4	C	-2.214	0.077	1247	4	O	-0.086	0.168	0.002
5	Cl	0.287	0.717	38.42	5	C	-1.786	0.020	206.4
6	C	1.445	0.027	1527	6	C	1.393	0.074	216.1
7	O	-0.227	1.072	3.069	7	C	1.395	0.005	40.54
8	C	-1.379	3.290	658.4	8	C	-1.052	0.002	30.81
9	Cl	0.287	0.042	13.40	9	C	-1.086	0.441	37.86
10	Cl	0.336	0.105	37.58	10	C	0.935	0.022	5.714
11	H	0.177	0.020	0.278	11	H	0.159	0.001	0.066
12	H	0.285	0.024	0.006	12	H	0.162	0.000	0.050
13	H	0.177	0.017	0.292	13	H	0.247	0.000	0.079

Table S10. The acute toxicity, chlorination toxicity and CHO cell cytotoxicity of TCP and TBP and some of their transformation products during chlorination with the presence of goethite, the acute toxicity, chlorination toxicity dates were calculated by ECOSAR software.

Compounds	Acute toxicity (mg/L)			Chronic toxicity (mg/L)			CHO cytotoxicity (LC ₅₀) (mol/L)	References
	Fish (LC ₅₀)	Daphnid (LC ₅₀)	Algae (EC ₅₀)	Fish	Daphnid	Algae		
2,4,6-TCP	2.728	1.564	6.252	0.340	0.297	2.844	2.44×10^{-4}	[13,14]
2,4,6-TBP	1.260	1.002	3.730	0.175	0.190	1.784	9.99×10^{-5}	[13,14]
OP6-175.94	172.0	131.8	153.7	124.0	0.306	23.68	1.12×10^{-5}	[14,15]
OP7-191.94	1198	846.1	783.5	1572	0.650	80.79	9.06×10^{-5}	[16]
OP12-265.84	391.1	295.7	326.0	322.4	0.533	45.91	1.44×10^{-5}	[16]
OP14-281.84	2649	1885	1615	3976	1.102	152.2	5.04×10^{-5}	[13,14,17,18]
OP15-241.87	2.175	1.391	5.429	0.281	0.264	2.496	1.75×10^{-4}	[13]
TCM	264.1	143.4	89.00	24.50	12.37	21.12	9.62×10^{-3}	[14]
TCAL	22.37	54.08	68.69	4.660	6.771	20.78	1.16×10^{-3}	[14,19]
DCAL	52.05	199.1	205.3	15.58	20.95	50.76	2.92×10^{-5}	[14,19]
TCA	22.37	54.08	68.69	4.660	6.771	20.78		
TBM	320.8	178.6	122.8	30.65	16.51	30.80	3.96×10^{-3}	[14]
BDCM	318.1	175.7	116.7	30.10	15.86	28.74	1.15×10^{-2}	[14]
DBCM	301.2	165.0	106.0	28.21	14.55	25.60	5.36×10^{-3}	[14]
TBAL	30.83	65.19	87.99	5.778	8.585	28.24	3.58×10^{-6}	[14,19]

References

- [1] F. Dong, Q. Lin, J. Deng, T. Zhang, C. Li, X. Zai, Impact of UV irradiation on *Chlorella* sp. damage and disinfection byproducts formation during subsequent chlorination of algal organic matter, *Sci. Total Environ.* 671 (2019) 519-527.
- [2] F. Dong, C. Li, X. Ma, Q. Lin, G. He, S. Chu, Degradation of estriol by chlorination in a pilot-scale water distribution system: Kinetics, pathway and DFT studies, *Chem. Eng. J.* 383 (2020).
- [3] F. Dong, C. Li, J. Crittenden, T. Zhang, Q. Lin, G. He, W. Zhang, J. Luo, Sulfadiazine destruction by chlorination in a pilot-scale water distribution system: Kinetics, pathway, and bacterial community structure, *J. Hazard. Mater.* 366 (2019) 88-97.
- [4] S. Fukahori, H. Ichiura, T. Kitaoka, H. Tanaka, Capturing of bisphenol A photodecomposition intermediates by composite TiO₂-zeolite sheets, *Appl. Catal., B* 46(3) (2003) 453-462.
- [5] N. Gao, W. Chu, Y. Deng, S. W. Krasner, Precursors of Dichloroacetamide, an Emerging Nitrogenous DBP Formed during Chlorination or Chloramination, *Environ. Sci. Technol.* 44(10) (2010) 3908-3912.
- [6] H. Wang, C. Hu, X. Hu, M. Yang, J. Qu, Effects of disinfectant and biofilm on the corrosion of cast iron pipes in a reclaimed water distribution system. *Water Res.* 2012, 46(4): 1070-1078.
- [7] G.V. Buxton, C.L. Greenstock, W.P. Helman, A.B. Ross, Critical Review of rate constants for reactions of hydrated electrons, hydrogen atoms and hydroxyl radicals ($\bullet\text{OH}/\bullet\text{O}^-$) in Aqueous Solution, *J. Phys. Chem. Ref. Data* 17(2) (1988) 513-886.
- [8] D.M. Bulman, S.P. Mezyk, C.K. Remucal, The impact of pH and irradiation wavelength on the production of reactive oxidants during chlorine photolysis, *Environ. Sci. Technol.* 53(8) (2019) 4450-4459.
- [9] P. Sun, T. Meng, Z. Wang, R. Zhang, H. Yao, Y. Yang, L. Zhao, Degradation of organic micropollutants in UV/NH₂Cl advanced oxidation process, *Environ. Sci. Technol.* 53(15) (2019) 9024-9033.
- [10] K. Hasegawa, P. Neta, Rate constants and mechanisms of reaction of chloride (Cl_2^-) radicals, *J. Phys. Chem.* 82(8) (1978) 854-857.
- [11] K. Guo, Z. Wu, C. Shang, B. Yao, S. Hou, X. Yang, W. Song, J. Fang, Radical Chemistry and Structural Relationships of PPCP Degradation by UV/Chlorine Treatment in Simulated Drinking Water, *Environ. Sci. Technol.* 51(18) (2017) 10431-10439.
- [12] P. O'Neill, S. Steenken, D. Schulte-Frohlinde, Formation of radical cations of methoxylated benzenes by reaction with OH radicals, Ti^{2+} , Ag^{2+} , and $\text{SO}_4^{\bullet-}$ in aqueous solution. An optical and conductometric pulse radiolysis and in situ radiolysis electron spin resonance study, *J. Phys. Chem.* 79(25) (1975) 2773-2779.
- [13] Z. Zhang, Q. Zhu, C. Huang, M. Yang, J. Li, Y. Chen, B. Yang, X. Zhao, Comparative cytotoxicity of halogenated aromatic DBPs and implications of the corresponding developed QSAR model to toxicity mechanisms of those DBPs: Binding interactions between aromatic DBPs and catalase play an important role, *Water Res.* 170 (2020) 115283.
- [14] E.D. Wagner, M.J. Plewa, CHO cell cytotoxicity and genotoxicity analyses of disinfection by-products: An updated review, *J. Environ. Sci. China* 58 (2017) 64-76.

- [15] E. Prochazka, B.I. Escher, M.J. Plewa, F.D. Leusch, In Vitro Cytotoxicity and Adaptive Stress Responses to Selected Haloacetic Acid and Halobenzoquinone Water Disinfection Byproducts, *Chem. Res. Toxicol.* 28(10) (2015) 2059-68.
- [16] W. Wang, Y. Qian, J. Li, B. Moe, R. Huang, H. Zhang, S.E. Hrudey, X. Li, Analytical and toxicity characterization of halo-hydroxyl-benzoquinones as stable halobenzoquinone disinfection byproducts in treated water, *Anal. Chem.* 86(10) (2014) 4982-8.
- [17] M.J. Plewa, J.E. Simmons, S.D. Richardson, E.D. Wagner, Mammalian cell cytotoxicity and genotoxicity of the haloacetic acids, a major class of drinking water disinfection by-products, *Environ. Mol. Mutagen.* 51(8-9) (2010) 871-8.
- [18] M.J. Plewa, Y. Kargalioglu, D. Vancker, R.A. Minear, E.D. Wagner, Mammalian cell cytotoxicity and genotoxicity analysis of drinking water disinfection by-products, *Environ. Mol. Mutagen.* 40(2) (2002) 134-42.
- [19] C. Jeong, C. Postigo, S. Richardson, J. Simmons, S. Kimura, B. Marinas, D. Barcelo, P. Liang, E. Wagner, M. Plewa, Occurrence and Comparative Toxicity of Haloacetaldehyde Disinfection Byproducts in Drinking Water, *Environ. Sci. Technol.* 49(23) (2015) 13749-59.